

RUBBER LATEX VESSEL DETECTION FROM MICROSCOPIC CROSS-SECTION IMAGES

Miss Jirapath Jariyawatthananon



จุฬาลงกรณ์มหาวิทยาลัย

CHULALONGKORN UNIVERSITY

A Thesis Submitted in Partial Fulfillment of the Requirements

for the Degree of Master of Science Program in Computer Science and Information

Technology

Department of Mathematics and Computer Science

Faculty of Science

Chulalongkorn University

Academic Year 2013

บทคัดย่อและแฟ้มข้อมูลฉบับเต็มของวิทยานิพนธ์ตั้งแต่ปีการศึกษา 2554 ที่ให้บริการในคลังปัญญาจุฬาฯ (CUIR)

Copyright of Chulalongkorn University

เป็นแฟ้มข้อมูลของนิสิตเจ้าของวิทยานิพนธ์ ที่ส่งผ่านทางบัณฑิตวิทยาลัย

The abstract and full text of theses from the academic year 2011 in Chulalongkorn University Intellectual Repository (CUIR) are the thesis authors' files submitted through the University Graduate School.

การตรวจหาท่อลำเลียงน้ำจากภาพตัดขวางที่ได้จากกล้องจุลทรรศน์



นางสาวจิรภัทร์ จริยาวัฒนานนท์

จุฬาลงกรณ์มหาวิทยาลัย

CHULALONGKORN UNIVERSITY

วิทยานิพนธ์นี้เป็นส่วนหนึ่งของการศึกษาตามหลักสูตรปริญญาวิทยาศาสตรมหาบัณฑิต
สาขาวิชาวิทยาการคอมพิวเตอร์และเทคโนโลยีสารสนเทศ ภาควิชาคณิตศาสตร์และวิทยาการ
คอมพิวเตอร์

คณะวิทยาศาสตร์ จุฬาลงกรณ์มหาวิทยาลัย

ปีการศึกษา 2556

ลิขสิทธิ์ของจุฬาลงกรณ์มหาวิทยาลัย

Thesis Title	RUBBER LATEX VESSEL DETECTION FROM MICROSCOPIC CROSS-SECTION IMAGES
By	Miss Jirapath Jariyawatthananon
Field of Study	Computer Science and Information Technology
Thesis Advisor	Assistant Professor Rajalida Lipikorn, Ph.D.

Accepted by the Faculty of Science, Chulalongkorn University in Partial
Fulfillment of the Requirements for the Master's Degree

.....Dean of the Faculty of Science
(Professor Supot Hannongbua, Dr.rer.nat.)

THESIS COMMITTEE

.....Chairman
(Assistant Professor Nagul Cooharajanane, Ph.D.)

.....Thesis Advisor
(Assistant Professor Rajalida Lipikorn, Ph.D.)

.....External Examiner
(Assistant Professor Gun Srijuntongsiri, Ph.D.)

จุฬาลงกรณ์มหาวิทยาลัย
CHULALONGKORN UNIVERSITY

จิรภัทร์ จริยาวัฒนานนท์ : การตรวจหาท่อลำเลียงน้ำยางจากภาพตัดขวางที่ได้จากกล้องจุลทรรศน์. (RUBBER LATEX VESSEL DETECTION FROM MICROSCOPIC CROSS-SECTION IMAGES) อ.ที่ปรึกษาวิทยานิพนธ์หลัก: ผศ. ดร. รัชลิดา ลิปิกรณ์, 62 หน้า.

งานวิจัยนี้นำเสนอวิธีการตรวจหาและคัดแยกท่อน้ำยาง จากภาพตัดขวางโตนสีเทา โดยงานวิจัยนี้นำเสนอเทคนิค พหุนามการปรับเส้นโค้ง โดยใช้จุดสูงสุดและต่ำสุดของจุดหนึ่ง เทคนิคพหุนามการปรับเส้นโค้ง ใช้ในการตรวจหาตำแหน่งของท่อน้ำยางจากรูปภาพตัดขวางที่ไม่ได้ย้อมสีที่ถ่ายโดยกล้องถ่ายภาพดิจิทัลผ่านกล้องจุลทรรศน์ จากนั้นท่อน้ำยางได้ถูกคัดแยกออกจากรูปภาพโดยใช้จุดสูงสุดและต่ำสุดของจุดหนึ่ง และการปฏิบัติการเชิงสัญญาณวิทยาแบบปิด. ในการทดลองครั้งนี้ได้ใช้ต้นยางสองสายพันธุ์เป็นตัวอย่างในการทดลอง ได้แก่พันธุ์ RRIM600 และ พันธุ์ RRIT251 ในแต่ละพันธุ์ใช้ตัวอย่างจากลำต้นของต้นยาง อายุ 1-2 ปี พันธุ์ละ 30 รูปภาพตัดขวางจากผลการทดลองที่ปรากฏ พบว่างานวิจัยฉบับนี้สามารถตรวจหาและคัดแยกท่อน้ำยางได้อย่างตรงจุดและถูกต้อง



จุฬาลงกรณ์มหาวิทยาลัย
CHULALONGKORN UNIVERSITY

ภาควิชา คณิตศาสตร์และวิทยาการ
คอมพิวเตอร์

ลายมือชื่อนิสิต

ลายมือชื่อ อ.ที่ปรึกษาวิทยานิพนธ์หลัก

สาขาวิชา วิทยาการคอมพิวเตอร์และ
เทคโนโลยีสารสนเทศ

ปีการศึกษา 2556

ACKNOWLEDGEMENTS

I would like to greatly thank my thesis advisor, Assistant Professor Dr. Rajalida Lipikorn for giving me advices and always helps me when I got a trouble. She also encourages and put an effort on me which helps me to complete and finish my thesis. I am really appreciate and want to thank you my advisor for this valuable time for 3 years.

And I want to acknowledge Dr. Manit Kidyoo from department of Botany who gave me the knowledge about rubber trees and their structure. Moreover, he also allowed me to use all the necessary equipment in botanic laboratory for the experiments.

Finally, I would like to thank you my family especially my parents who always support everything to me.



CONTENTS

	Page
THAI ABSTRACT	iv
ENGLISH ABSTRACT	v
ACKNOWLEDGEMENTS	vi
CONTENTS	vii
LIST OF TABLES	ix
LIST OF FIGURES	x
CHAPTER I.....	1
Introduction	1
1.1. Objectives.....	4
1.2. Scope of the Work.....	4
1.3. Problem Formulation.....	4
1.4. Expected Outcomes.....	5
CHAPTER II.....	6
Related Work and Theoretical Background	6
2.1. Related Work	6
2.2. Detection and Segmentation	7
2.2.1. Polynomial Curve Fitting.....	8
2.2.2. Stationary points.....	9
2.3. Image Enhancement	11
2.3.1. Dilation.....	14
2.3.2. Erosion	17
2.3.3. Closing.....	19
CHAPTER III.....	20
Proposed Method and Implementation.....	20
3.1. Image Pre-processing	21
3.2. Rubber latex vessel detection and segmentation.....	23
Experimental Results and Discussion.....	28

	Page
CHAPTER V	34
Conclusion	34
REFERENCES	35
APPENDICES.....	36
APPENDIX A.....	37
APPENDIX B.....	43
APPENDIX C.....	47
VITA.....	62



จุฬาลงกรณ์มหาวิทยาลัย
CHULALONGKORN UNIVERSITY

LIST OF TABLES

	PAGE
Table 1: Rules for Dilation and Erosion for binary image.....	14
Table 2: The percentage of accuracy.....	29
Table 3: The result of proposed method	29
Table 4: The comparison result of RRIM600 and RRIT251	32



LIST OF FIGURES

	PAGE
Figure 1: Original image of RRIM600 rubber tree cross-section.....	2
Figure 2: Original image of RRIT251 rubber tree cross-section.....	2
Figure 3: Structure of rubber tree trunk cross-section.....	3
Figure 4: Hevea brasiliensis or rubber tree.....	3
Figure 5: Example of Polynomial Curve Fitting.....	8
Figure 6: local maximum stationary point.....	10
Figure 7: local maximum stationary point.....	10
Figure 8: Diamond shape structuring element.....	12
Figure 9: Disk shape structuring element.....	12
Figure 10: Line shape structuring element.....	13
Figure 11: Octagon shape structuring element.....	13
Figure 12: Morphological dilation of a grayscale image.....	15
Figure 13: (a) Original Input grayscale image, (b) Output grayscale image after apply dilation operation.....	16
Figure 14: (a) Original Input binary image, (b) Output binary image after apply dilation operation.....	17
Figure 15: (a) Original Input grayscale image, (b) Output grayscale image after apply erosion operation.....	18
Figure 16: (a) Original Input binary image, (b) Output binary image after apply erosion operation.....	18
Figure 17: (a) Original Input binary image, (b) Output binary image after apply closing operation.....	19
Figure 18: The process of the proposed methods.....	20
Figure 19: (a) Original input RGB image, (b) Gray scale image.....	21
Figure 20: (a) Image before enhanced by histogram equalization, (b) image after enhanced by histogram equalization, (c): result image using 4-neighbor connected component.....	22
Figure 21: Final result of image pre-processing.....	22

Figure 22: (a) Extract the pixel intensities of first column, (b) First column extraction, (c) Pixel intensities plot of first column.....	24
Figure 23: Polynomial intensity curve-fitting.....	24
Figure 24: Minimum and maximum stationary points	25
Figure 25: (a) The area of rubber latex vessel, (b) The segmented area of rubber latex vessel, (c) The segmented area of rubber latex vessels result	26
Figure 26: The results after apply all columns.....	26
Figure 27: The result of morphological closing operation	27
Figure 28 - 83: Original images of experimental data and the results of proposed method.....	48

CHAPTER I

Introduction

Rubber trees or formally called *Hevea brasiliensis* are one of the most important economic plants of many countries whose latex can be used to produce variety of rubber products such as rubber gloves, rubber bands, flat tire and many more. It is necessary and very important that the harvesters should have not only the knowledge about how to grow rubber trees but also the structures of rubber latex vessels so that they can estimate the volume of rubber latex that will be produced from each species. Different species of rubber trees usually have different rubber latex vessel structures which is invisible from outside. Since the rubber latex vessels are very small and cannot be seen by the naked eyes, we have to cut through a rubber tree trunk and use a microscope to look at the cross-section of a trunk. According to Figures 1-2, the structure of a rubber tree trunk is very complex and contains many different components which are very similar and difficult to distinguish rubber latex vessels from other components. A trunk normally has three layers: bark, cambium, and wood. A microscopic cross-sectional image in Figure 1 shows only two layers of a trunk which are bark and cambium and the rubber latex vessels are located in the inner layer of the bark next to the cambium layer as seen in Figure 3.

A microscopic cross-section image of a rubber tree trunk can be used to analyze rubber latex vessels because it contains several features that can be used to distinguish the vessels from other components. These features include color, shape, and texture. In order to create a 3D structure of rubber latex vessels to see the appearance and characteristics of rubber tree which using for a tapping process, the detection of the rubber latex vessels region is necessary. Therefore, the objective of this thesis is to detect and segment rubber latex vessels from microscopic cross-section images using the above-mentioned features. Two species of rubber trees of age between one to two years old are used in the experiments namely, RRIM600 and

RRIT251, and the cross-section slices are cut from stems with diameter approximately no more than one centimeter. The images of non-dyed cross-section slices of two species taken by a digital camera through microscope lens are shown in Figures 1-2.

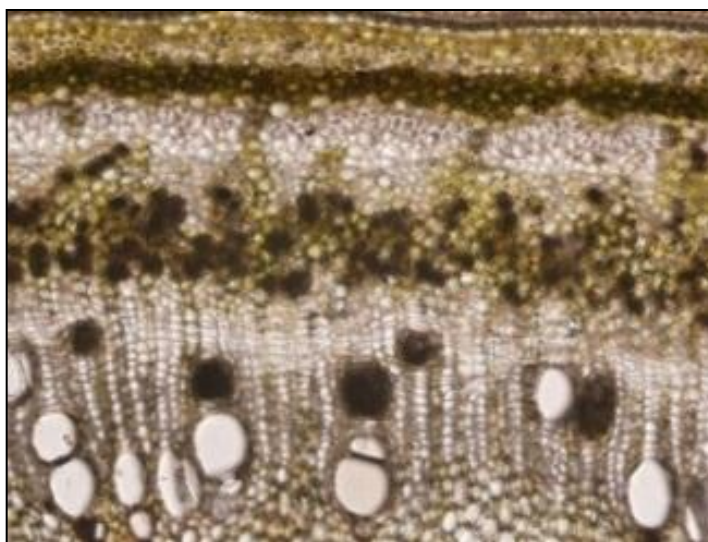


Figure 2: Original image of RRIT251 rubber tree cross-section

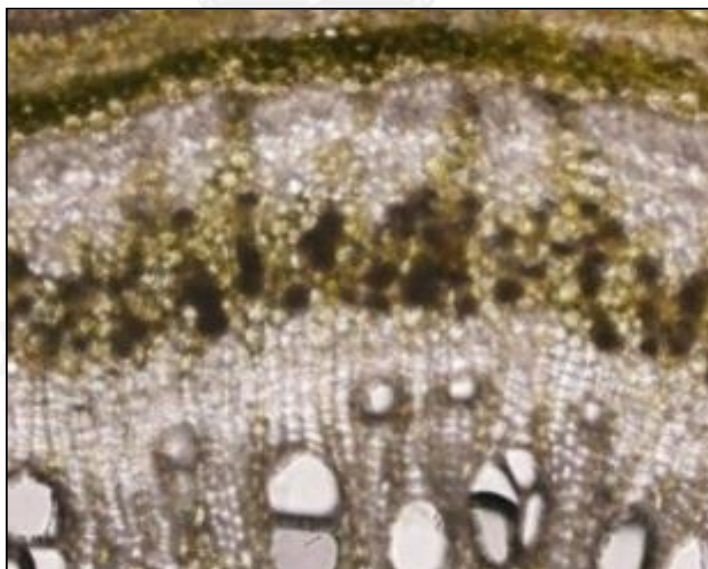


Figure 1: Original image of RRIM600 rubber tree cross-section

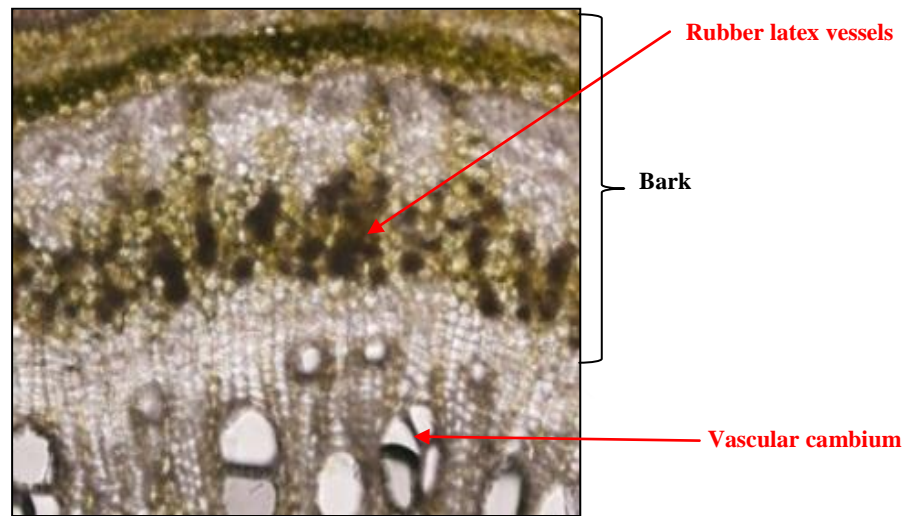


Figure 3: Structure of rubber tree trunk cross-section



Figure 4: *Hevea brasiliensis* or rubber tree

1.1. Objectives

To detect and segment rubber latex vessel area from the microscopic cross-section image of a trunk of a rubber tree.

1.2. Scope of the Work

In this research, the detection system is constrained as follows:

1. Detect and segment the areas of the rubber latex vessels from microscopic cross-section images.
2. Enhance the areas of rubber latex vessels.
3. Use microscopic images with 20x magnification of non-dyed rubber tree cross-section images
4. File Extension .jpg
5. 1-2 year-old rubber trees
6. 2 rubber tree species; RRIM600 and RRIT251

1.3. Problem Formulation

To detect and segment the areas of rubber latex vessels are quite difficult because the structure and texture of the rubber tree is complex. Each layer or component of rubber tree is very similar and this is the major problem of detecting and segmenting the rubber latex vessel areas.

There is no other researches that detect and segment this kind of images before, thus this would be a challenge to find the method that can detect and separate the areas of rubber latex vessels from rubber tree cross-section images.

Cross-section images used in the experiments are cut and the pictures were taken from equipment in botany department laboratory. It takes amount of time to learn how to use this equipment. Therefore, the quality of images firstly is not quite good yet but for a while the quality is better and suitable for using in this experiment.

1.4. Expected Outcomes

- The proposed methods can detect and segment the area of rubber latex vessels.
- The detection and segmentation of rubber latex vessels are improved by the proposed method.



CHAPTER II

Related Work and Theoretical Background

In this chapter, the related work and theoretical background has been described. In related work is described about the related techniques used for detection and segmentation an image. Next, all the techniques that have been used in this thesis are shown in the theory and the background information to give the understanding of each technique.

2.1. Related Work

There are various image processing techniques used in botanical and agricultural areas, especially in segmentation, texture analysis, feature extraction, thresholding is the most widely used technique in object segmentation. Some curve-fitting techniques are also used in segmenting an object as well but mostly used together with edge detection. One of the techniques used in texture classification and object extraction is called Gray Level Co-occurrence Matrix (GLCM) which analyzes texture for all directions (for example 0, 45, and 90 degree). To extract an object from the RGB input image, GLCM is used together with color segmentation and two-dimension OTSU thresholding [1, 2] . Although, OTSU is widely used in segmentation an object but this technique is effective on the image that the segmented object is obviously different from the background and the other component in an image. In order to classify the texture, various kinds of images have been used as an input such as Brodatz textures or Microscopic images. Normalized GLCM is used to extract the features and K-Nearest Neighbor (K-NN) is used to classify the texture [3]. This texture analysis works properly when analyze the pure texture image which no other components included but not for our input images because the texture of all components are very similar and difficult to distinguish.

Curve-fitting can be used to segment an object by extracting the edges of an object first then combining with other segmentation techniques such as color segmentation and curvature-based curve searching and finally, curve-fitting or least-square curve fitting is used to segment an object [4, 5]. These two researches use least-square curve fitting technique which is the simplest and common to find the best fit of the data. They use microscopic image and RGB image as an input data which uncomplicated object. These methods are effectively with the edged data.

Another presented segmentation method is to use texture, thresholding, and morphological operations. Entropy function of gray scale image and thresholding are used to segment an object and morphological operators such as dilation, thinning and filling are used to extract the final result [6, 7]. Mathematical morphology has been used in many areas and work properly with most kinds of images. Morphological Operators can be used not only for image enhancement but also for object detection [8]. But morphological operators cannot be used to detect rubber latex vessels but to effectively enhance an image instead.

Sarvaiya, J.N., et al. described image registration by template matching based on normalized cross-correlation (NCC) using Cauchy-Schwartz's inequality. An NCC algorithm checks and calculates the small image or template matches to which position on the original image [9]. However, none of these techniques can be used to detect and segment rubber latex vessels because the texture of a rubber tree trunk is very delicate and difficult to distinguish.

2.2. Detection and Segmentation

The main objective of this thesis is to propose the methods for rubber latex vessels detection and segmentation. There are two main techniques: polynomial curve-fitting and morphological closing operation. Polynomial curve-fitting is used to detect the location of rubber vessels. Then rubber latex vessels are segmented from an image using maximum and minimum stationary points and finally, the rubber latex vessels are enhanced by morphological closing operation. The detail of these techniques is as follows:

2.2.1. Polynomial Curve Fitting

Curve Fitting is used to find the best fit curve for a given data set. In this thesis we use polynomial curve fitting to detect the rubber latex vessel regions from intensity value. An example of polynomial curve fitting of 4th degree and 5th degree is shown in Figure 5.

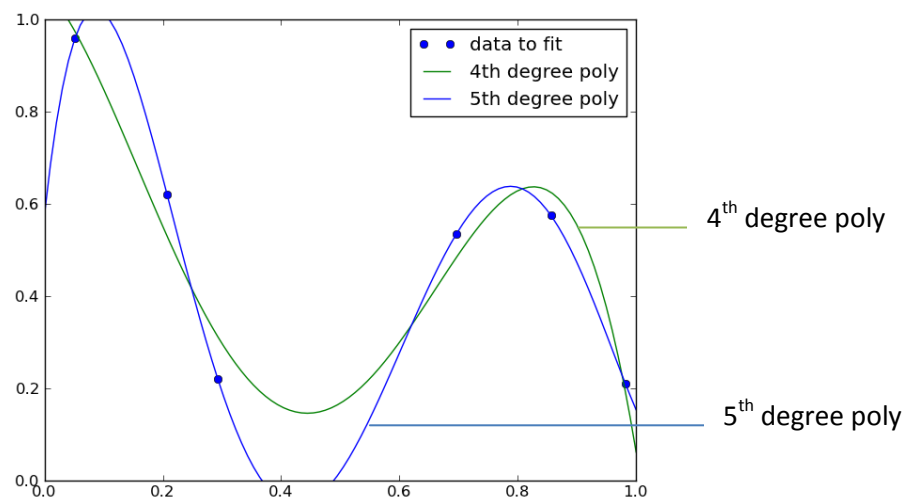


Figure 5: Example of Polynomial Curve Fitting

Polynomial intensity curve fitting means finding the curve that best fits the intensities of an image using polynomial. Let $f(x,y)$ represent an input image, (x,y) represent coordinates of each pixel, and $f(x)$ represent intensity of any pixel from each column of an image. The **nth-order** polynomial intensity curve fitting can be written as

$$p(x) = c_1x^n + c_2x^{n-1} + \dots + c_nx + c_{n+1}$$

where the coefficient, c_j , of the polynomial can be calculated from

$$\sum_{j=1}^{n+1} \left(\sum_{i=1}^M x_i^{2n+2-j-k} \right) c_j = \sum_{i=1}^M x_i^{n+1-k} f(x_i)$$

Deviation of the intensity curve from each data point is

$$e_i = f(x_i) - p(x_i), \quad i = 1, \dots, M$$

where M is the number of pixels in each column. By using least square error, $\frac{\partial E}{\partial c_j} = 0, j = 1, \dots, n + 1$ such that E is the sum of the squared deviations:

$$E = \sum_{i=1}^M e_i^2$$

2.2.2. Stationary points

Stationary point, x_0 , is a local maximum or local minimum point on a curve where the derivative is zero. If drawing a tangent line along the curve, the point at which the tangent line parallel to x-axis is a local minimum or maximum point which can be defined as:

$$y = f(x_0) \text{ at which } \left. \frac{df}{dx} \right|_{x_0} = 0$$

Figures 6 and 7 show the curve with local minimum and local maximum

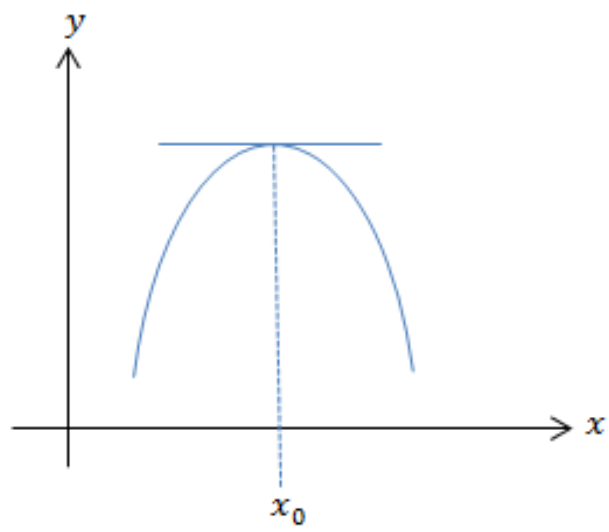


Figure 6: local maximum stationary point

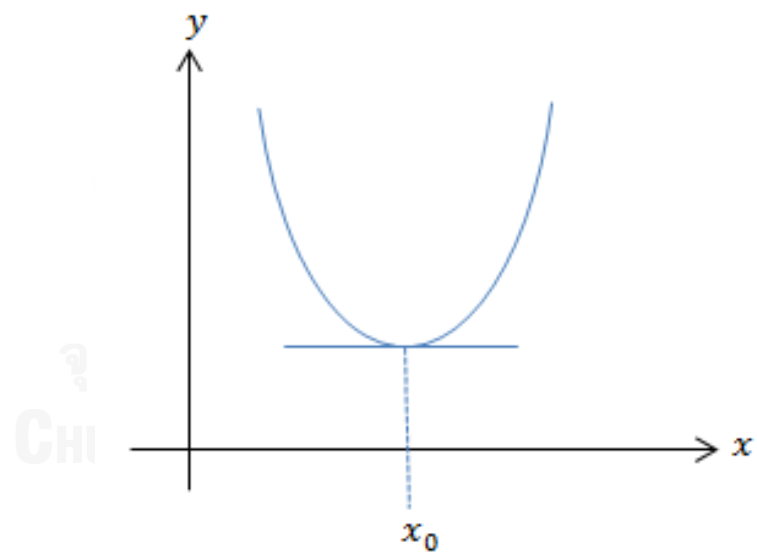


Figure 7: local minimum stationary point

2.3. Image Enhancement

One of the most widely used techniques in image enhancement is called mathematical morphology. This technique can be applied to both binary and grayscale images. Morphology in image processing is the enhancement process based on shape. Morphological operation works with an image by apply a structuring element which is a small shape or a template to an input image. The structuring element is positioned at each pixel on an input image and then it is compared the corresponding pixels with its neighbors and produce an output image with the same size.

Basically, there are two morphological operations that are widely used in processing an image, dilation and erosion. Dilation is a technique that adds pixels to object boundaries in an image. On the other hand, erosion is a technique that removes pixels from object boundaries in an image. For both operations, the number of adding or removing pixels depends on the shape and size of structuring element.

Structuring element is a set of matrices consists of pixel 0 and 1, which 1 is defined as neighborhood. There are two types of structuring element, two-dimensional or flat and three-dimensional or non-flat. Two-dimensional structuring element has a center pixel called an origin which indicates the interest pixel of structuring element. But for three-dimensional structuring element will adds the height for the third dimension. The shapes of two-dimensional element are arbitrary, diamond, line, disk, octagon, periodocline, rectangle, pair, and square. The shapes of three-dimensional structuring element are arbitrary and ball.

Following are examples of structuring elements:

We can define the size of the structuring element which calculates from the origin of structuring element. Below examples the size is equal to 3 which calculate from the origin.

- Diamond shape structuring element

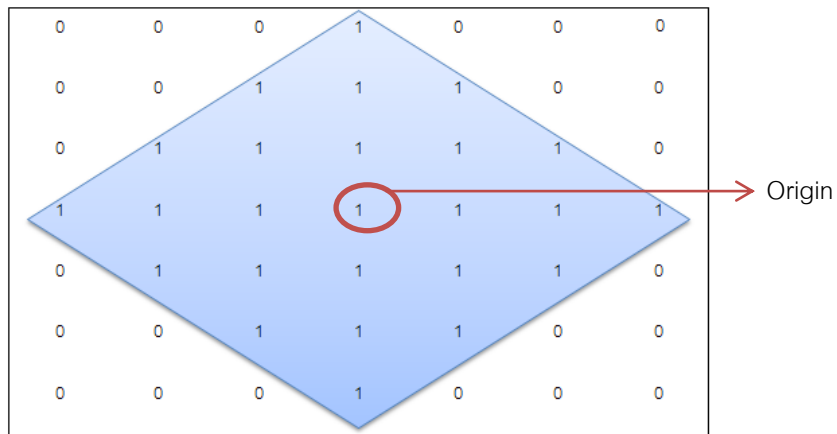


Figure 8: Diamond shape structuring element

- Disk shape structuring element

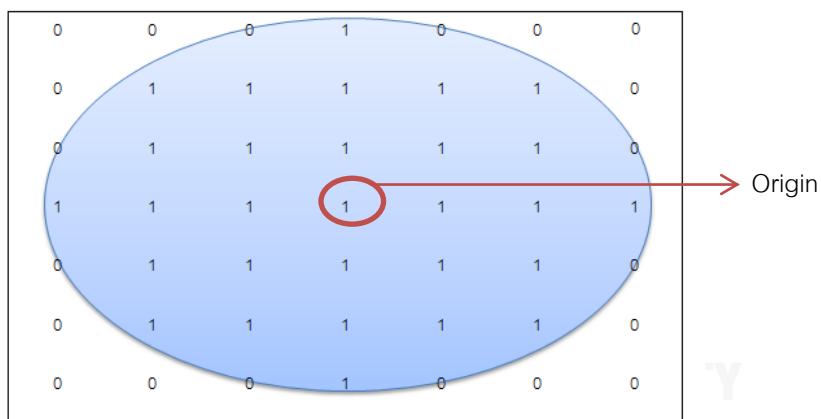


Figure 9: Disk shape structuring element

- Line shape structuring element

For line shape, it has a length instead of a size which calculates from the first neighborhood of the structuring element until the last one. Another thing that line shape is different to others is a degree, Figure 10 shows that this line shape has 0 degree and the length equal to 9.

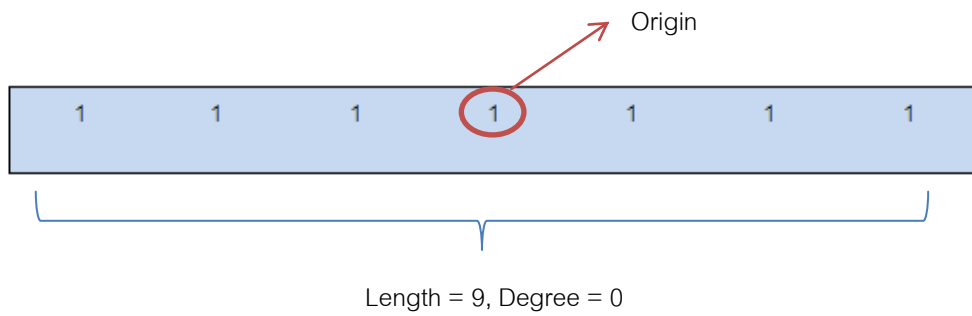


Figure 10: Line shape structuring element

- Octagon shape structuring element

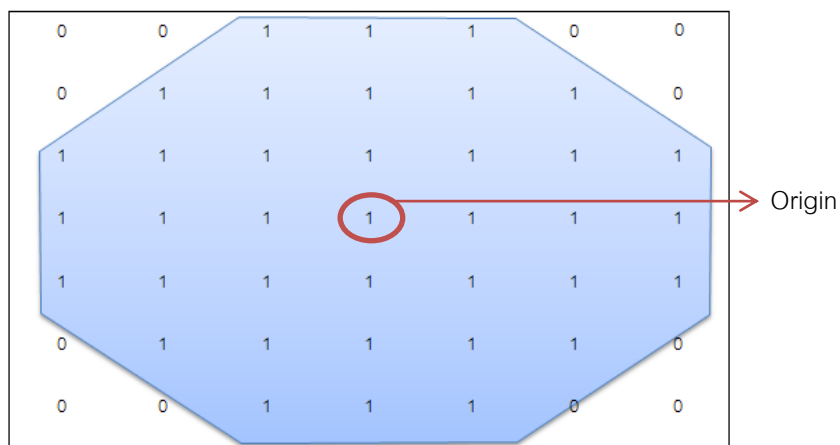


Figure 11: Octagon shape structuring element

Table 1: Rules for Dilation and Erosion for binary image

Operation	Rule
Dilation	The output pixel value is the <i>maximum</i> value of all the pixels in the neighborhood. In a binary image, if any of the neighbor pixels has intensity value equals to 1, then the output pixel is set to 1.
Erosion	The output pixel value is the <i>minimum</i> value of all the pixels in the neighborhood. In a binary image, if any of the neighbor pixels has intensity equals to 0, then the output pixel is set to 0.

2.3.1. Dilation

Figure 12 shows the process of dilation on a grayscale image.

The process shows how the structuring element defines the output value of a particular pixel in an input grayscale image; the maximum or highest pixel value of all the pixels in the neighborhood is considered as the corresponding output pixel by choosing the maximum value to be the output value. From Figure 12, 14 is a particular pixel and the highest neighborhood pixel of a particular value is 15 then the output pixel value is 15.

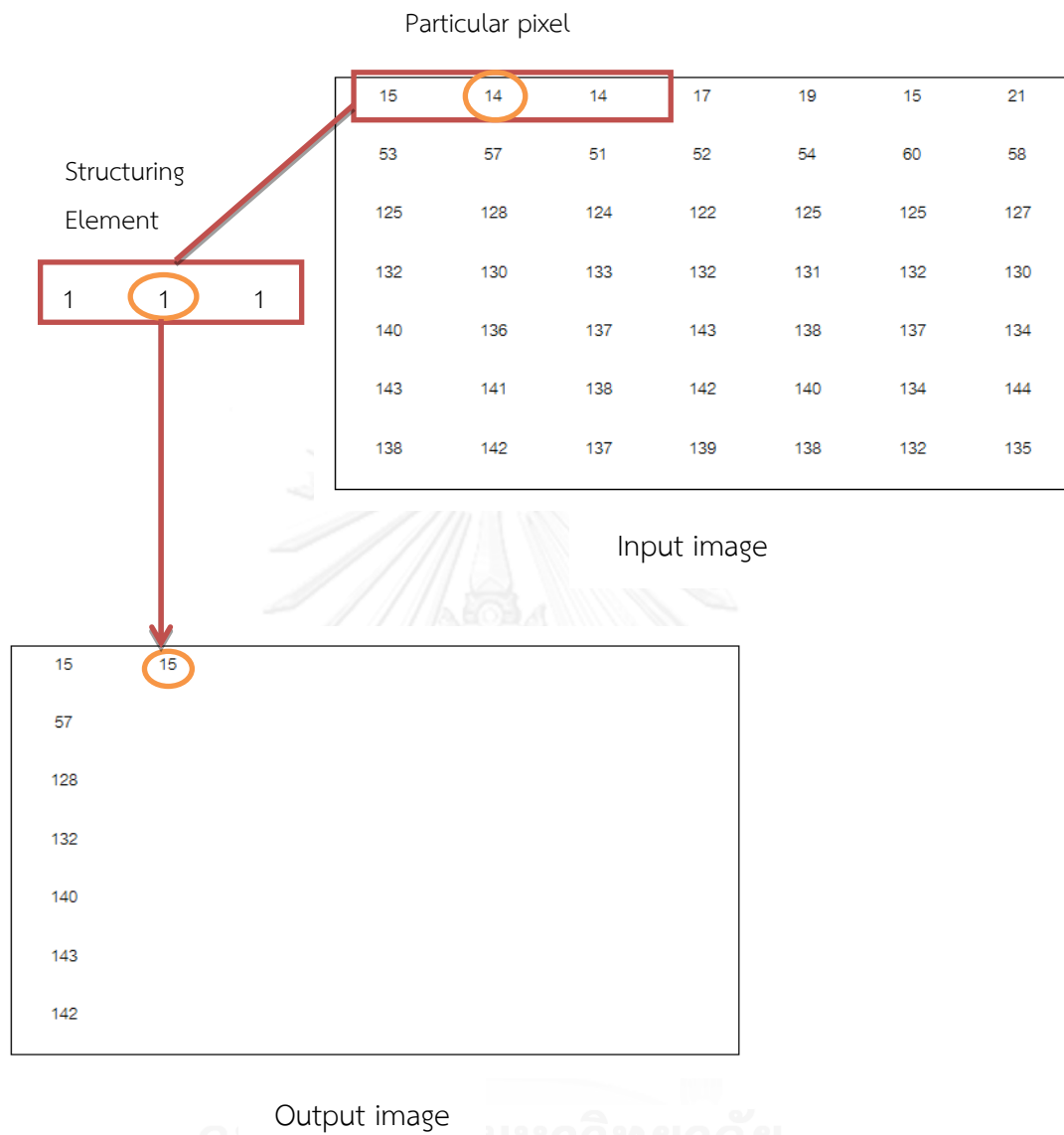


Figure 12: Morphological dilation of a grayscale image

Dilation of a gray image $A(x, y)$ by a structuring element $B(x, y)$, denoted by $A \oplus B$, can be written as:

$$(A \oplus B)(x, y) = \max\{A(x - x', y - y') + B(x', y') \mid (x', y') \in D_B\}$$

where D_B is a domain of structure element B .

Figure 13 shows an example of dilation operation on a grayscale image with a ball shape structuring element.



Figure 13: (a) Original Input grayscale image, (b) Output grayscale image after apply dilation operation

Figure 14 shows an example of dilation operation on a binary image with a vertical line structuring element.

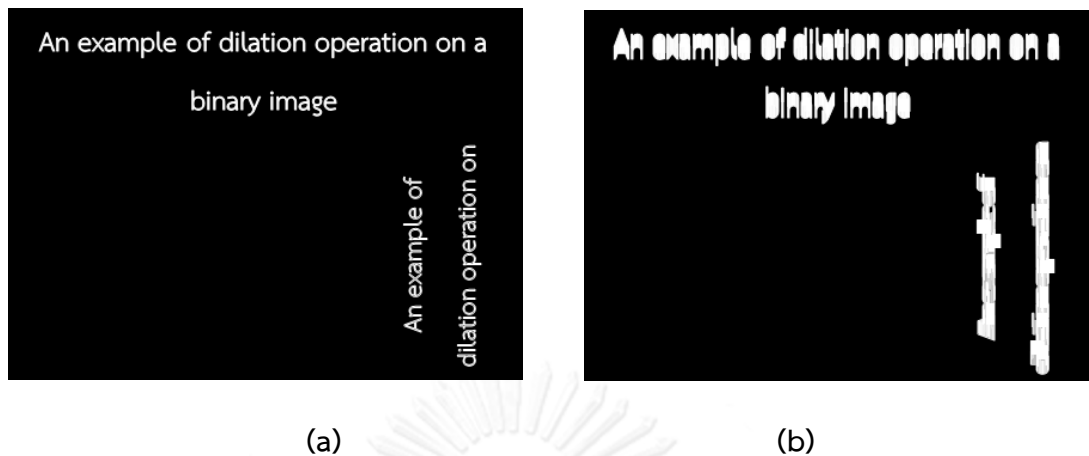


Figure 14: (a) Original Input binary image, (b) Output binary image after apply dilation operation

2.3.2. Erosion

Erosion is opposite from dilation in the way that an output pixel value comes from the minimum value among a particular pixel and its neighborhood.

Erosion of a gray image $A(x, y)$ by a structuring element $B(x, y)$, denoted by $A \ominus B$, can be written as:

$$(A \ominus B)(x, y) = \min\{A(x + x', y + y') - B(x', y') \mid (x', y') \in D_B\}$$

where D_B is a domain of structure element B .

Figure 15 shows an example of erosion operation on a grayscale image with a disk shape structuring element.



Figure 15: (a) Original Input grayscale image, (b) Output grayscale image after apply erosion operation

Figure 16 shows an example of erosion on a binary image with a disk structuring element.

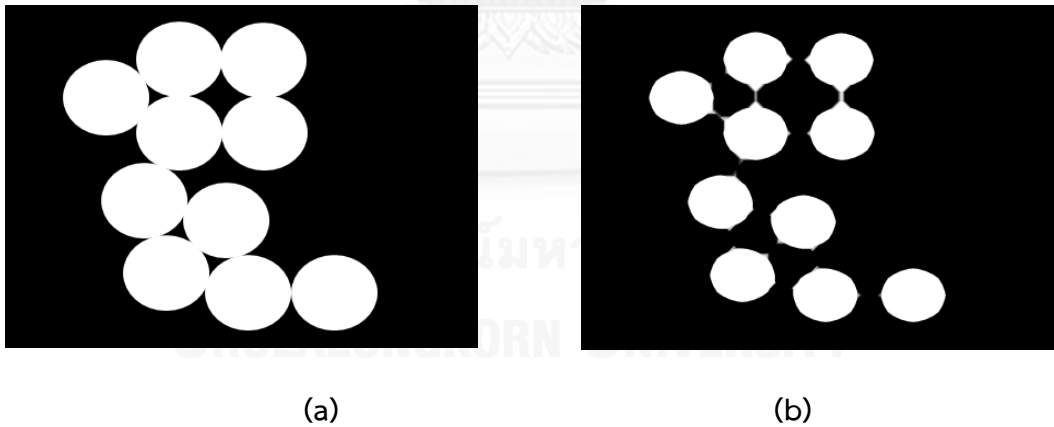


Figure 16: (a) Original Input binary image, (b) Output binary image after apply erosion operation

2.3.3. Closing

Closing is a combination of dilation and erosion where the process starts with dilation and followed by erosion using the same structuring element for both operations.

Closing of an image $A(x,y)$ by a structuring element $B(x,y)$, denoted by $A \bullet B$, is an operation of dilation followed by erosion and can be written as:

$$A \bullet B = (A \oplus B) \ominus B$$

Figure 17 shows an example of using closing operation to fill gaps of an object in a binary image.

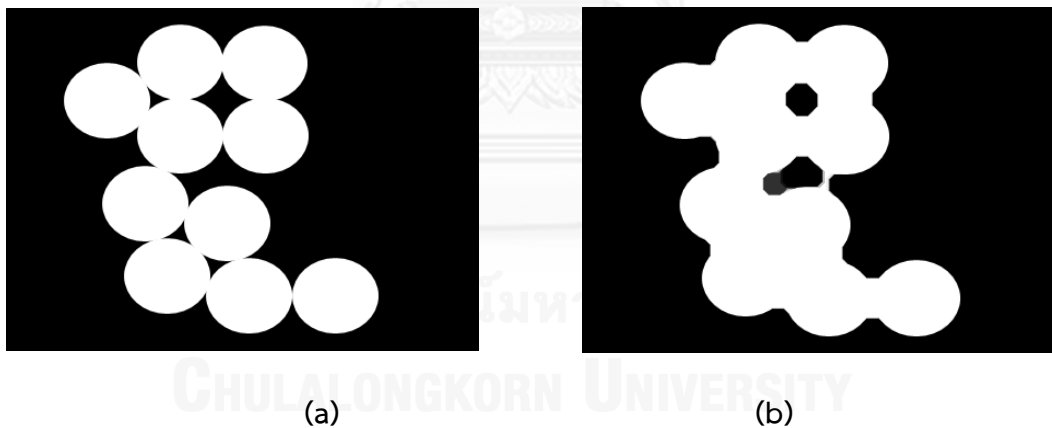


Figure 17: (a) Original Input binary image, (b) Output binary image after apply closing operation

CHAPTER III

Proposed Method and Implementation

The new methods for rubber latex vessels detection and segmentation using polynomial intensity curve-fitting and stationary points are proposed in this thesis. The proposed methods consist of the following steps (as shown in Figure 18):

- 1) An input image pre-processing.
- 2) Rubber latex vessel regions detection and segmentation using polynomial intensity curve-fitting together with maximum and minimum stationary points.
- 3) The segmented rubber latex vessel regions enhancement using morphological closing operations.

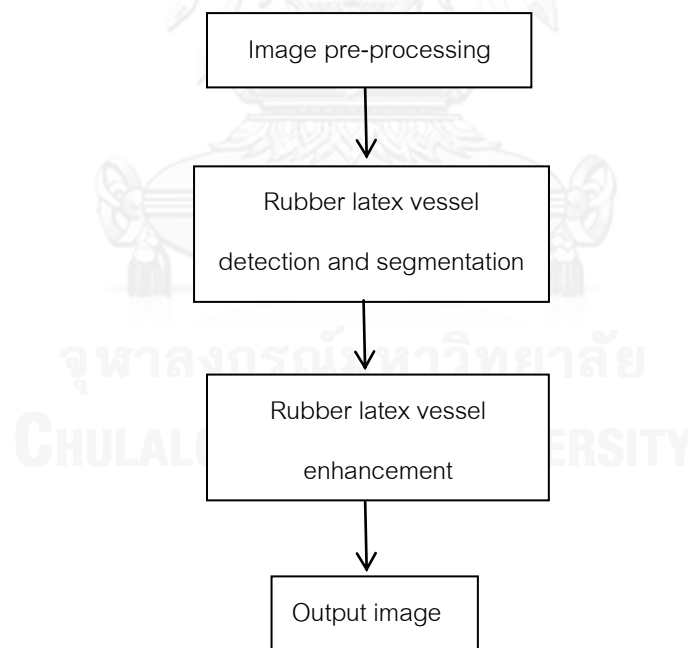


Figure 18: The process of the proposed methods

3.1. Image Pre-processing

In the first step, the original RGB image, which was taken from real sample with digital equipment, is resized and converted to a gray scale image as shown in Figure 19.

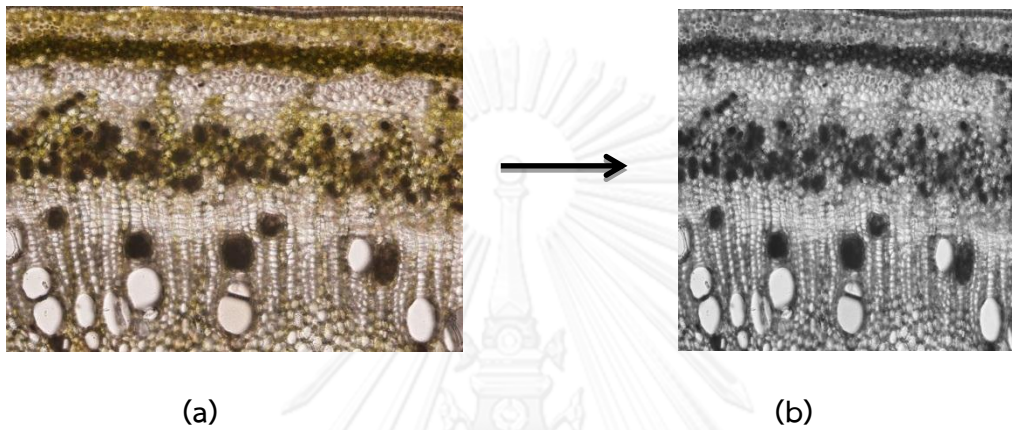
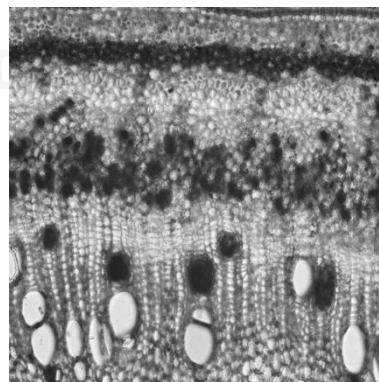


Figure 19: (a) Original input RGB image, (b) Gray scale image

The quality of an image is then enhanced by histogram equalization, whereas some artifacts and irrelevant components such as cambium and the bark surface are removed from an image by applying 4-neighbor connected component technique [10] to Figure 20 where the two main components: bark and rubber latex vessels area are the largest connected component otherwise has been removed.



(a)

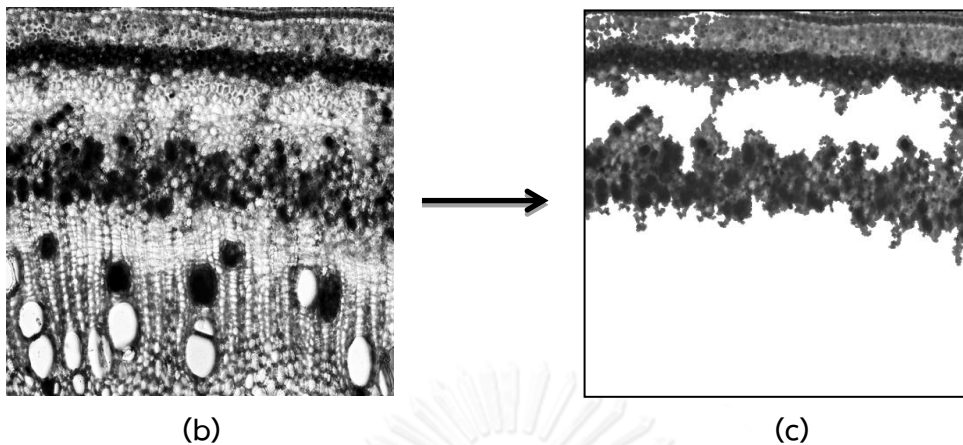


Figure 20: (a) Image before enhanced by histogram equalization, (b) image after enhanced by histogram equalization, (c): result image using 4-neighbor connected component

From the microscopic image in Figure 3, we can see that the structure of a rubber tree's stem contains two main components: the sparse area (bark and cambium) and the dense area (bark surface, rubber latex vessels). The sparse areas are removed by discarding any connected components that are small or their average intensities are higher than the global average intensity (average intensity of the whole image), and the result is shown in Figure 21. After removing sparse areas, it can be seen that the dense areas, which composed of rubber latex vessels and bark surface, are very similar thus they need to be segmented in the next step.

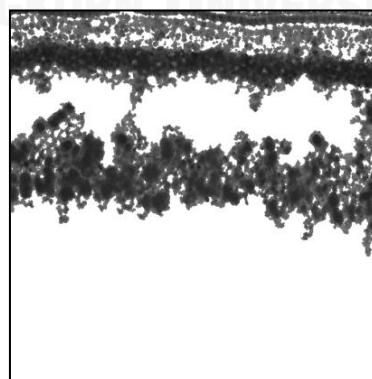
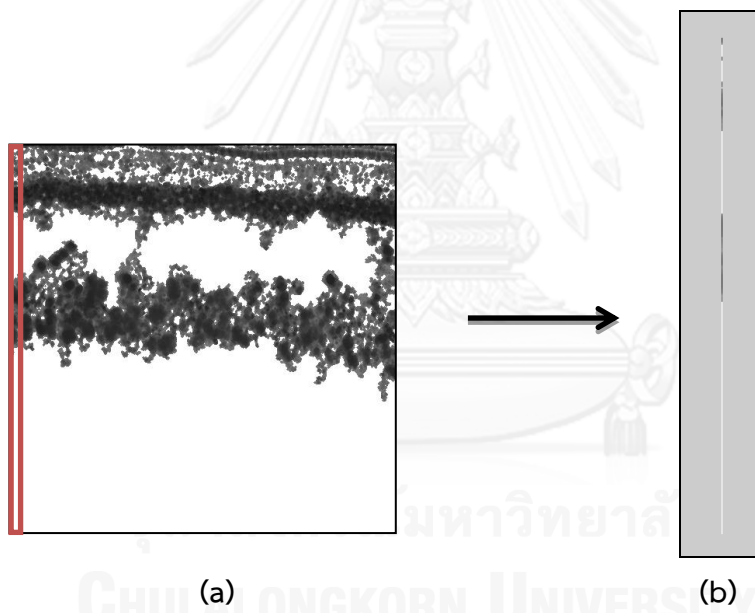


Figure 21: Final result of image pre-processing

3.2. Rubber latex vessel detection and segmentation

In this step, we combine polynomial intensity curve fitting with both minimum and maximum stationary points to detect and segment rubber latex vessels. The detection of rubber latex vessels is performed column by column, starting from the first column and the process is as follows:

1. Extract the intensities of pixels along the first column. From Figure 22, since the image pre-processing result has only the bark surface and the rubber latex vessels area left, there are two major low intensity data group of the bark surface and rubber latex vessels, respectively.



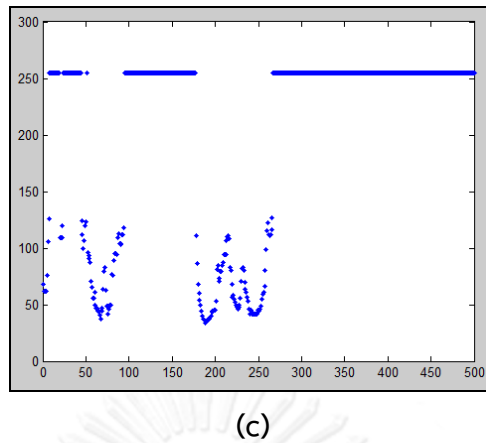


Figure 22: (a) Extract the pixel intensities of first column, (b) First column extraction, (c) Pixel intensities plot of first column

2. Use the polynomial intensity curve fitting to find the best curve that fits the data as shown in Figure 23.

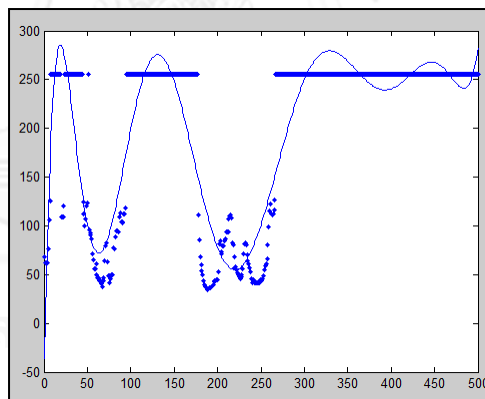


Figure 23: Polynomial intensity curve-fitting

3. Find the lists of minimum stationary points whose values are less than the average intensity of the column and the maximum stationary points whose values are greater than the average intensity of the column together with their coordinates as shown in Figure 24.

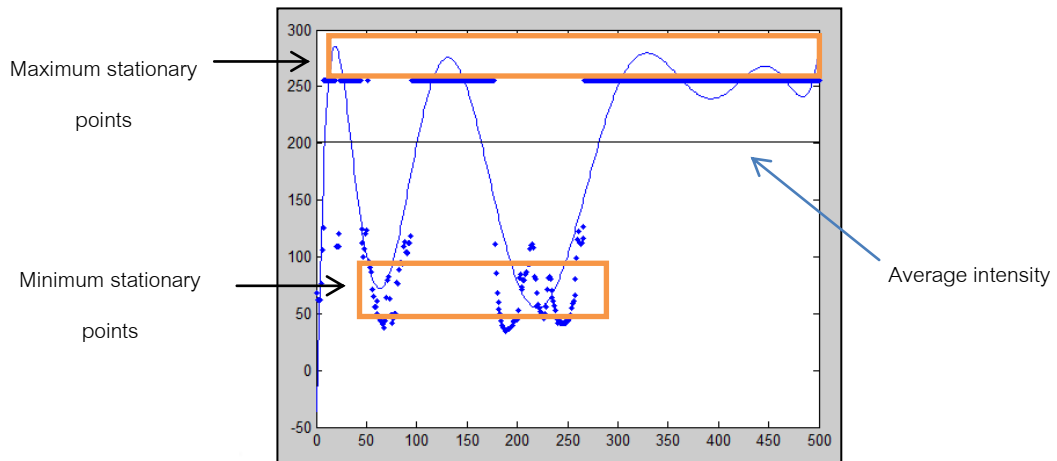
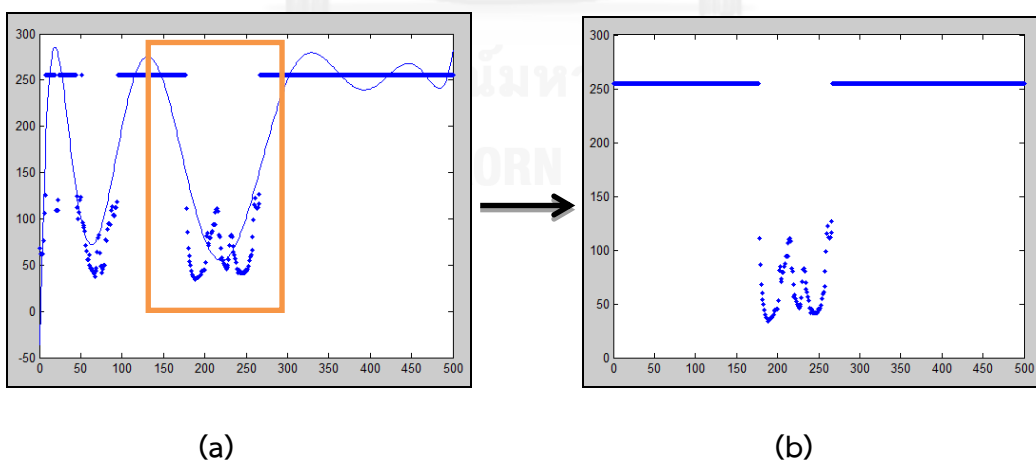


Figure 24: Minimum and maximum stationary points

4. Detect and segment rubber latex vessels by selecting the curve segment whose minimum stationary point obtained from step 3 is the right innermost because rubber latex vessels of the preprocessed image are located in the right innermost layer from the bark surface. Once, the rubber latex vessels are detected, other regions are converted to background color. The segmented region from the graph is shown in Figure 25(a)-(b) and the rubber latex vessels corresponding to the segmented region are shown in Figure 25(c).



(a)

(b)

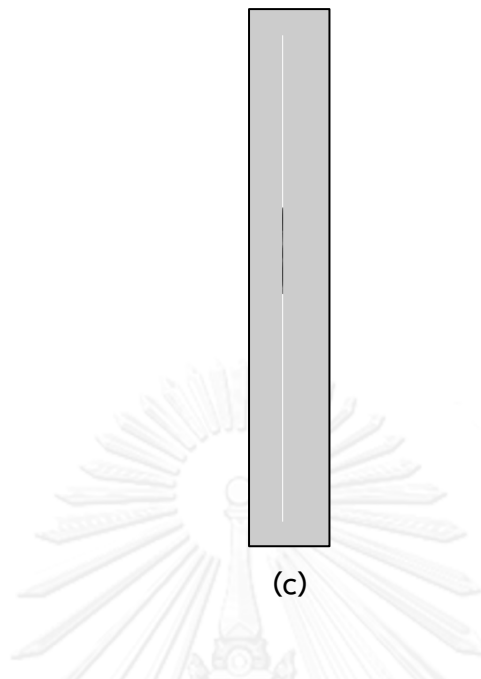


Figure 25: (a) The area of rubber latex vessel, (b) The segmented area of rubber latex vessel, (c) The segmented area of rubber latex vessels result

5. Apply the same process to the rest of the columns in an image and the result is shown in Figure 26. All the rubber latex vessel regions are obtained together with some artifacts, so the result will be enhanced and also artifacts will be removed in the next step.

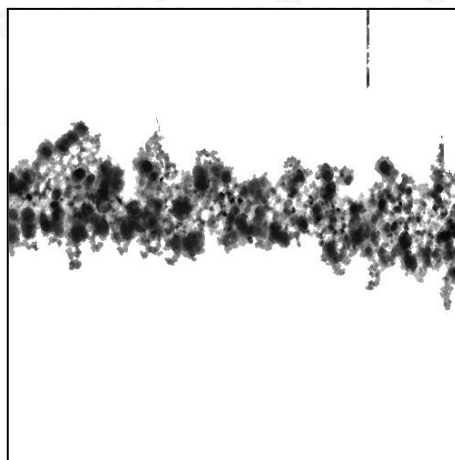


Figure 26: The results after apply all columns

3.3. Image Enhancement

The remaining artifacts are removed and the output image in Figure 26 is enhanced using morphological closing operation with a 5x5 disk shape structuring element and the result is shown in Figure 27, and it can be seen that the artifacts have been removed. The rubber latex vessels become more obvious and clearer.

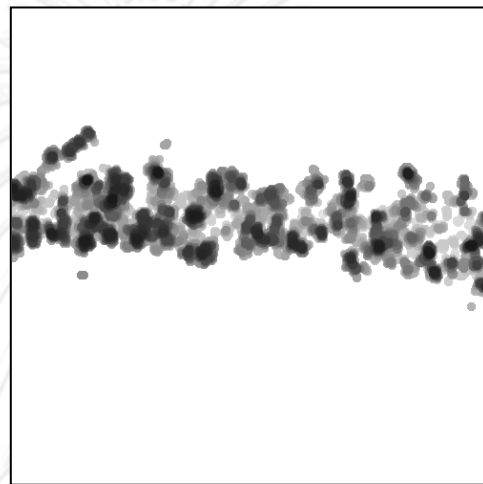


Figure 27: The result of morphological closing operation

CHAPTER IV

Experimental Results and Discussion

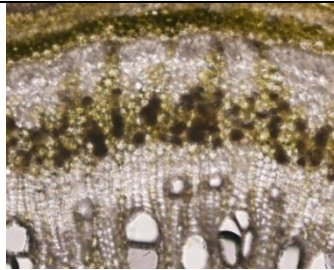
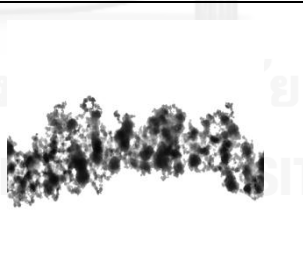
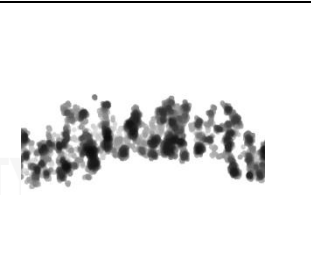
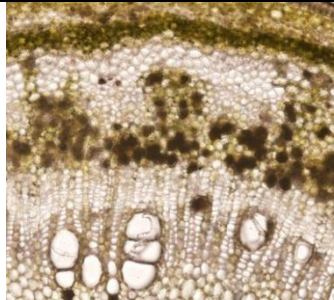
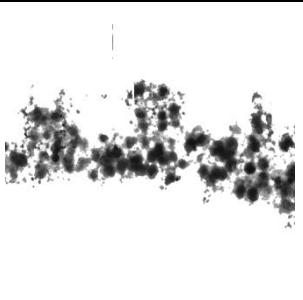
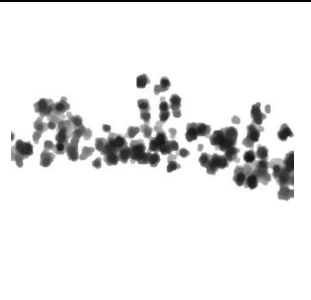
Two species of rubber trees, RRIM600 and RRIT251 with age between one to two years old whose non-dyed cross-sectional slices were cut from a stem with diameter approximately no more than one centimeter and image extension of .jpg and two data sets contain 30 microscopic cross-section images are used in the experiment. Polynomial curve-fitting with degree 10 are used to find the best curve to fit the data whereas the other degrees don't align and fit to the data at all. The results reveal that the proposed methods can detect and segment rubber latex vessel regions from most of the test images. An accuracy in correct detection is inspected by one specialist professor in rubber tree. There are some reasons for incorrect detection in some test images are from the differences of contrast in input images, it effects in the process of wrong detection and segmentation and some of test images, the texture of the cambium is very similar to that of the rubber latex vessels. Table 2 below shows the percentage of accuracy in detection and segmentation of rubber latex vessel regions. Table 3 shows example results after detection and segmentation process and the final results after applying morphological operations. Moreover, the results are useful for the prediction of the amount of latex vessels for each species which help to increase the harvesters' product and profit. Table 4 shows the comparison the amount of rubber latex vessels between RRIM600 and RRIT251.

Table 2: The percentage of accuracy

Rubber tree species	Number of correct detection and segmentation	Number of wrong detection and segmentation	Percentage of accuracy
RRIT251	27	3	90%
RRIM600	28	2	93.33%

Table 3 below shows example results of the proposed method. The table includes original images and the data name and species, the result of detection and segmentation and the result of image enhancement by morphological operations.

Table 3: The result of proposed method

Data species and name	Original image	Detection and Segmentation result	Final result with Morphological operations
RRIM600 (1rm.jpg)			
RRIM600 (4rm.jpg)			

RRIM600 (11rm.jpg)			
RRIM600 (26rm.jpg)			
RRIM600 (29rm.jpg)			
RRIT251 (rt1.jpg)			

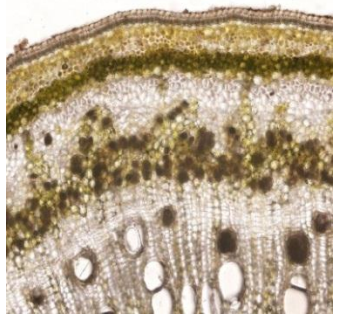
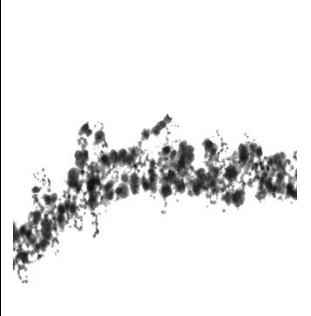

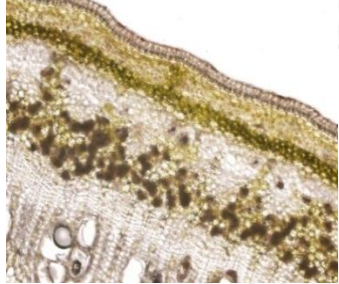


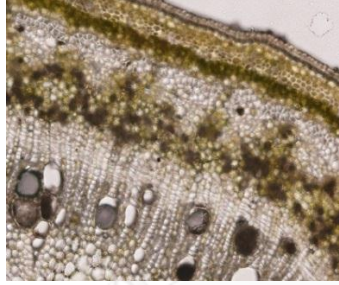
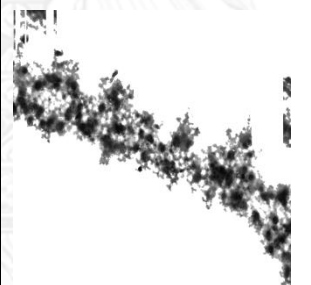
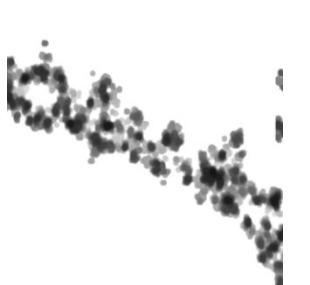
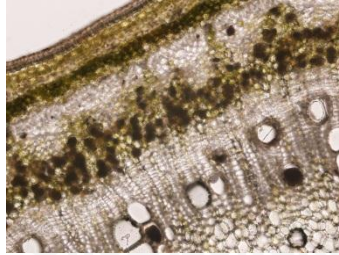
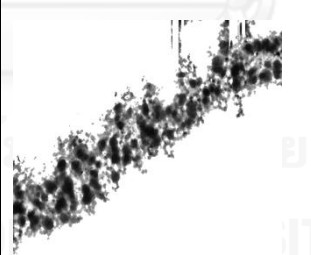
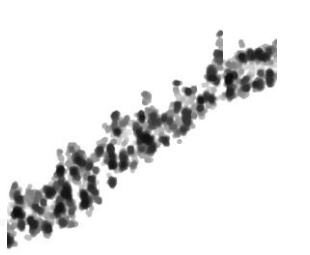
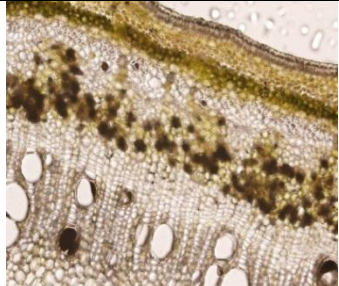
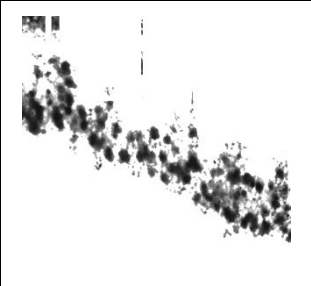

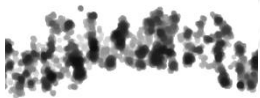
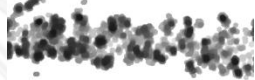



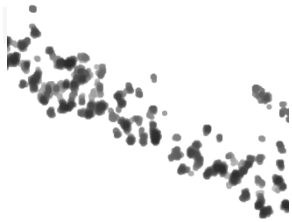
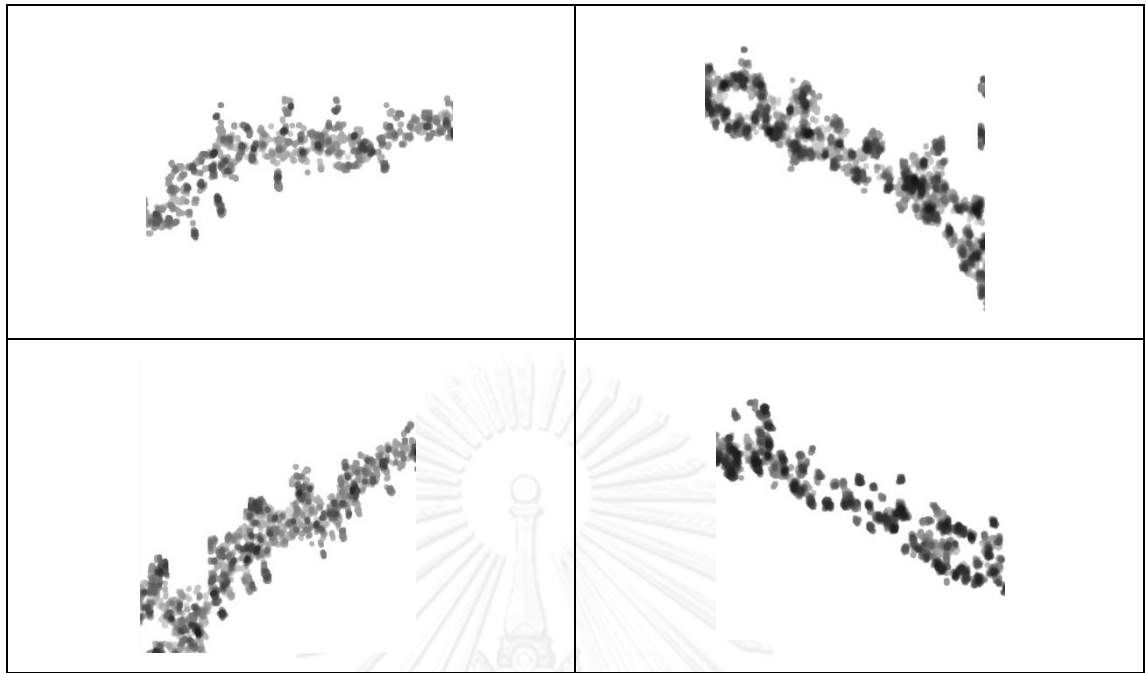
RRIT251 (rt3.jpg)			
RRIT251 (rt4.jpg)			
RRIT251 (rt7.jpg)			
RRIT251 (rt9.jpg)			
RRIT251 (rt21.jpg)			

Table 4 compare the result that show amount of rubber latex vessels between RRIM600 and RRIT251. Mostly, RRIT251 has more rubber latex vessels than RRIM600 which can be seen from the dark spots from the results.

Table 4: The comparison result of RRIM600 and RRIT251

RRIM600	RRIT251
	
	
	



CHAPTER V

Conclusion

This thesis proposes the new methods to detect and segment rubber latex vessel regions based on polynomial intensity curve fitting together with local maximum and local minimum stationary points. The final results are then enhanced by morphological closing operation. The results in Table 2 show that the proposed methods yield high accuracy rate for both rubber tree species. The results in Table 3 show example of input data and output data after detection and segmentation and morphological process for each species that correctly detect and segment by our proposed method. The reasons that the proposed method cannot detect and segment all of the rubber latex vessel regions are because in some test images the contrast of input images that have been taken from and digital equipment are different and in some test images the texture of the cambium is very similar to that of the rubber latex vessels.

For future work, the 3D rubber latex vessels will be constructed from a set of cross-section slices to see the characteristics and structure of rubber tree used for tapping process and improves the better detection and segmentation technique.

REFERENCES

1. Xiaosong, W., H. Xinyuan, and F. Hui. A Color-Texture Segmentation Method to Extract Tree Image in Complex Scene. in Machine Vision and Human-Machine Interface (MVHI), 2010 International Conference on. 2010. Kaifeng, China.
2. Komorkiewicz, M. and M. Gorgon. Foreground object features extraction with GLCM texture descriptor in FPGA. in Design and Architectures for Signal and Image Processing (DASIP), 2013 Conference on. 2013. Cagliari.
3. Suresh, A. and K.L. Shunmuganathan, Image Texture Classification using Gray Level Co-Occurrence Matrix Based Statistical Features. European Journal of Scientific Research, 2012. **75**: p. 591-597.
4. Xiaomin, L., et al. Cell Segmentation Using Ellipse Curve Segmentation and Classification. in Information Science and Engineering (ICISE), 2009 1st International Conference on. 2009. Nanjing.
5. Wei, S., W. Lifang, and T. Ling. A Curve Fitting Based Image Segmentation Method. in Computer Science and Information Technology - Spring Conference, 2009. IACSITSC '09. International Association of. 2009. Singapore.
6. Chaudhari, A.K. and J.V. Kulkarni. Local entropy based brain MR image segmentation. in Advance Computing Conference (IACC), 2013 IEEE 3rd International. 2013. Ghaziabad.
7. Aqeel, A.F. and S. Ganesan. Retinal image segmentation using texture, thresholding, and morphological operations. in Electro/Information Technology (EIT), 2011 IEEE International Conference on. 2011. Mankato, MN.
8. Oprea, S., et al. Digital image processing applied in drugs industry for detection of broken aspirin tablets. in Electronics Technology, 2008. ISSE '08. 31st International Spring Seminar on. 2008. Budapest.
9. Sarvaiya, J.N., S. Patnaik, and S. Bombaywala. Image Registration by Template Matching Using Normalized Cross-Correlation. in Advances in Computing, Control, & Telecommunication Technologies, 2009. ACT '09. International Conference on. 2009. Trivandrum, Kerala.
10. Chapron, M., P. Boissard, and L. Assemat. A multiresolution based method for recognizing weeds in corn fields. in Pattern Recognition, 2000. Proceedings. 15th International Conference on. 2000. Barcelona.



APPENDICES

จุฬาลงกรณ์มหาวิทยาลัย
CHULALONGKORN UNIVERSITY



APPENDIX A

จุฬาลงกรณ์มหาวิทยาลัย
CHULALONGKORN UNIVERSITY

Lactiferous vessel detection from microscopic cross-sectional images

Jirapath Jariyawatthananon, Nagul Cooharajanone, Rajalida Lipikorn

Machine Intelligence and Multimedia Information Technology Laboratory
Department of Mathematics and Computer Science
Faculty of Science, Chulalongkorn University
Bangkok 10330, Thailand

Jirapath.J@student.chula.ac.th, Nagul.C@chula.ac.th, Rajalida.L@chula.ac.th

ABSTRACT

This paper presents the methods to detect and segment lactiferous vessels or rubber latex vessels from gray scale microscopic cross-sectional images using polynomial curve-fitting with maximum and minimum stationary points. Polynomial curve-fitting is used to detect the location of lactiferous vessels from an image of a non-dyed cross-sectional slice which was taken by a digital camera through microscope lens. The lactiferous vessels are then segmented from an image using maximum and minimum stationary points with morphological closing operation. Two species of rubber trees of age between one to two years old are sampled namely, RRDM600 and RRIT251. Two data sets contain 30 microscopic cross-sectional images of one-year old rubber tree's stems from each species are used in the experiments and the results reveal that most of the lactiferous vessel areas can be segmented correctly.

Keywords: lactiferous vessels, rubber latex vessels, image detection and segmentation, polynomial curve-fitting, stationary points

1. INTRODUCTION

Rubber trees or formally called *Hevea brasiliensis* are one of the most important economic plants whose latex can be used to produce variety of rubber products such as flat tire, rubber glove and many more. It is necessary and very important that the harvesters should have not only the knowledge about how to grow rubber trees but also the structure of lactiferous vessels so that they can estimate the volume of rubber latex that will be produced from each species. Different species of rubber trees usually have different lactiferous vessel structures which is invisible from outside. Since the lactiferous vessels are very small and cannot be seen by the naked eyes, we have to cut through a rubber tree trunk and use a microscope to look at the cross-section of a trunk. According to Figures 1-2, the structure of a rubber tree trunk is very complex and contains many different components which are very similar and difficult to distinguish lactiferous vessels from other components. A trunk normally has three layers: bark, cambium, and wood. A microscopic cross-sectional image in Figure 1 shows only two layers of a trunk which are bark and cambium and the lactiferous vessels are located in the inner layer of the bark next to the cambium layer as seen in Figure 3.

A microscopic cross-sectional image of a rubber tree trunk can be used to analyze lactiferous vessels because it contains several features that can be used to distinguish the vessels from other components. These features include color, shape, and texture. The objective of this paper is to detect and segment lactiferous vessels from microscopic cross-sectional images using the above-mentioned features. Two species of rubber trees of age between one to two years old are used in the experiments namely, RRDM600 and RRIT251, and the cross-sectional slices are cut from stems with diameter approximately no more than one centimeter. The images of non-dyed cross-section slices of two species taken by a digital camera through microscope lens are shown in Figures 1-2.

This paper is organized into the following sections: introduction is presented in section I, related work is described in section II then the proposed methods are presented in section III. Experimental results and conclusion are discussed in section IV and V, respectively.

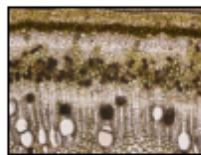


Figure1: Original image of RRJT251 rubber tree cross-section

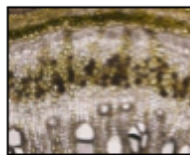


Figure2: Original Image of RRJM600 rubber tree cross-section

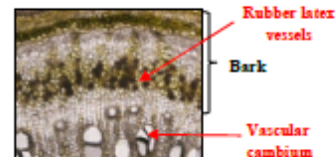


Figure3: Structure of rubber tree trunk cross-section

2. RELATED WORK

2.1. Literature review

Various image processing techniques have been used in botanical and agricultural areas, especially in segmentation, texture analysis, and feature extraction. One of the most famous texture analysis and feature extraction called Gray level co-occurrence matrix (GLCM) was combined with color, OTSU thresholding and connected component to extract an object [1] [2]. Normalized GLCM and K-Nearest Neighbor (K-NN) were used to classify texture [3]. Least-square curve-fitting have been used in object segmentation by combining with color feature and curvature-based curve [4] [5].

Another proposed segmentation method is to use texture, thresholding, and morphological operations. Entropy function of gray scale image and thresholding are used to segment an object and morphological operators are then used to extract the final result [6] [7]. Morphological Operators can also be used for object detection [8]. Sarvaiya, J.N., Patnaik, S., and Bombaywala, S. described image registration by template matching based on normalized cross-correlation (NCC) using Cauchy-Schwartz's inequality. An NCC algorithm will check and calculate that small image or template match to which position on the original image [9]. However, none of these techniques can be used to detect and segment lactiferous vessels because the texture of a rubber tree trunk is very delicate and difficult to distinguish.

2.2. Notion

The proposed methods adapt the properties of polynomial curve fitting and stationary points to detect and segment lactiferous vessels.

2.2.1. Polynomial intensity curve fitting: Let $f(x, y)$ represent an input image, (x, y) represent coordinates of each pixel, and $f(x)$ represent intensity of any pixel from each column of an image. The n -order polynomial intensity curve fitting can be written as

$$p(x) = c_0x^n + c_1x^{n-1} + \dots + c_nx + c_{n+1} \quad (1)$$

Deviation of the intensity curve from each data point is

$$\theta_i = f(x_i) - p(x_i), \quad i = 1, \dots, M \quad (2)$$

where M is the number of pixels in each column. By using least square error, $\frac{\partial E}{\partial c_j} = 0$, $j = 1, \dots, n + 1$ such that E is the sum of the squared deviations:

$$E = \sum_{i=1}^M \theta_i^2 \quad (3)$$

Equivalently, the coefficient, c_j , of the polynomial can be calculated from

$$\sum_{j=1}^{n+1} (\sum_{i=1}^M x_i^{2n+2-j-k}) c_j = \sum_{i=1}^M x_i^{n+1-k} f(x_i) \quad (4)$$

2.2.2. Stationary point, x_0 , is a local maximum or local minimum point on a graph where the derivative is zero which can be defined as:

$$y = f(x_0) \text{ at which } \frac{df}{dx} \Big|_{x_0} = 0 \quad (5)$$

In our proposed method, $f(x_0)$ represents the maximum or minimum intensity, and x_0 represents the x -coordinate of a pixel whose intensity is maximum or minimum.

2.2.3. Mathematical morphological operation

Dilation Operation –Dilation of a gray image A by a structuring element B , denoted by $A \oplus B$, can be written as:

$$(A \oplus B)(x, y) = \max\{A(x - x', y - y') + B(x', y') \mid (x', y') \in D_B\} \quad (6)$$

where D_B is a domain of structure element B .

Erosion Operation –Erosion of a gray image A by a structuring element B , denoted by $A \ominus B$, can be written as:

$$(A \ominus B)(x, y) = \min\{A(x + x', y + y') - B(x', y') \mid (x', y') \in D_B\} \quad (7)$$

where D_B is a domain of structure element B .

The Closing Operation – Closing of an image A by a structuring element B denoted by $A \bullet B$ is an operation of dilation followed by erosion and can be written as:

$$A \bullet B = (A \oplus B) \ominus B \quad (8)$$

3. PROPOSED METHOD

The new methods for lactiferous vessels detection and segmentation using polynomial intensity curve fitting and stationary points are proposed in this paper. The proposed method consists of the following steps(as shown in Figure 4): 1) preprocess an input image; 2) detect and segment lactiferous vessel regions using polynomial intensity curve fitting together with maximum and minimum stationary points; and 3) enhance the segmented lactiferous vessel regions using morphological operations.

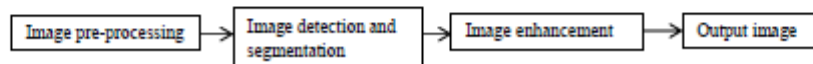


Figure 4: The process of the proposed method.

3.1. Pre-processing

In this step, the original RGB image, which was taken from real sample with digital equipment, is converted to a gray scale image. The quality of an image is then enhanced by histogram equalization, whereas some artifacts and irrelevant components such as cambium and the bark surface are removed from an image using 4-neighbor connected component. From the microscopic image in Figure 3, we can see that the structure of a stem contains two main components: the sparse area (bark and cambium) and the dense area (bark surface, lactiferous vessels). The sparse areas are removed by discarding any connected components that are small or their average intensities are higher than the

global average intensity (average intensity of the whole image) and the result is shown in Figure 4. It can be seen that the dense areas, which composed of lactiferous vessels and bark surface, are very similar thus they need to be segmented in the next step.

3.2. Detection and segmentation

In this step, we combine polynomial intensity curve fitting with stationary points to detect and segment lactiferous vessels. The detection of lactiferous vessels is performed column by column, starting from the first column and the process is as follows:

1. Extract the intensities of pixels along a column as shown in Figure 6.
2. Use the polynomial intensity curve fitting to find the best curve that fits the data as shown in Figure 7.
3. Find the lists of minimum stationary points whose values are less than the average intensity of the column and the maximum stationary points whose values are greater than the average intensity of the column together with their coordinates.
4. Detect and segment lactiferous vessels by selecting the curve segment whose minimum stationary point obtained from step 2 is the innermost because lactiferous vessels of the preprocessed image are located in the innermost layer from the bark surface. Once, the lactiferous vessels are detected, other regions are converted to background color. The segmented region from the graph is shown in Fig. 8 and the lactiferous vessels corresponding to the segmented region is shown in Fig. 9.

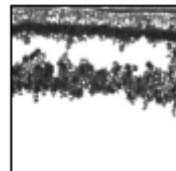


Figure 5: The result of pre-processing

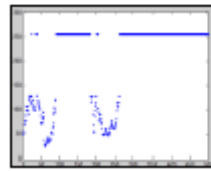


Figure 6: Graph of intensities of one column

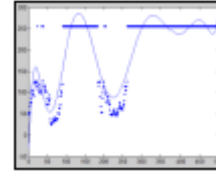


Figure 7: Polynomial intensity curve fitting graph

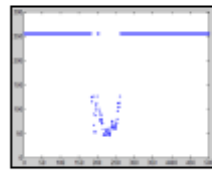


Figure 8: Result after segmentation by stationary points

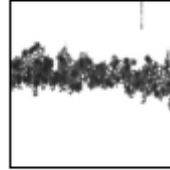


Figure 9: Result of lactiferous vessel region segmentation

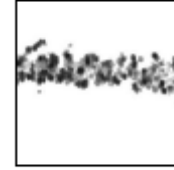


Figure 10: Final result of using closing morphological operation

5. Remove the remaining artifacts and enhance the output image using morphological closing operation with a 5x5 disk shape structuring element and the result is shown in Figure 10.

4. EXPERIMENTAL RESULTS

Two species of rubber trees, RRIM600 and RRIT251 with age between one to two years old whose cross-sectional slices were cut from a stem with diameter approximately no more than one centimeter are used in the

experiment. The results reveal that the proposed methods can detect and segment lactiferous vessel regions from most of the test images. Table 1 below shows the percentage of accuracy in detection and segmentation of lactiferous vessel regions.

Rubber tree species	Number of correct detection and segmentation	Number of wrong detection and segmentation	Percentage of accuracy
RRIT251	27	3	90%
RRIM600	28	2	93.33%

Table 1: The percentage of accuracy

5. CONCLUSION

This paper proposes the new methods to detect and segment lactiferous vessel regions based on polynomial intensity curve fitting together with local maximum and local minimum stationary points. The final results are then enhanced by morphological closing operation. The results in Table 1 show that the proposed methods yield high accuracy rate. The reasons that the proposed method cannot detect and segment all of the lactiferous vessel regions are because in some test images the lactiferous vessels are not connected or else they do not produce rubber latex and in some test images the texture of the cambium is very similar to that of the lactiferous vessels.

For future work, the 3D lactiferous vessels will be constructed from a set of cross-section slices to see the characteristics and structure of rubber tree used for tapping process.

References

- [1] Xiaosong Wang, Xinyuan Huang, and Hui Fu, "A Color-texture Segmentation Method to Extract Tree Image in Complex Scene," Proc. International Conference on Machine Vision and Human-machine Interface (MVHI), 621 – 625 (2010).
- [2] Komorkiewicz Mateusz, and Gorgon Mateusz, "Foreground objects features extraction with GLCM texture descriptor in FPGA," Proc. Design and Architectures for Signal and Image Processing (DASIP), 157-164 (2013).
- [3] A. Suresh, and K. L. Shunmuganathan, "Image Texture Classification using Gray Level Co-Occurrence Matrix Based Statistical Features," European Journal of Scientific Research, vol.75(4), 591-597 (2012).
- [4] Wei Shen, Lifang Wu, and LingTu, "A curve fitting based image segmentation method," Proc. International Association of Computer Science and Information Technology - Spring Conference (IACSITSC), 71-75 (2009).
- [5] Xiaomin Li, Yuanyuan Wang, Yinhui Deng, and Jinhua Yu, "Cell segmentation using ellipse curve segmentation and classification," Proc. The 1st International Conference on Information Science and Engineering (ICISE), 1187 – 1190 (2009).
- [6] Chaudhari, A.K. and Kulkarni, J. V., "Local Entropy based Brain MR Image Segmentation," Proc. IEEE International Advance Computing Conference (IACC), 1229 - 1233 (2013).
- [7] Aqeel, A.F. and Ganesan, S., "Retinal Image Segmentation using Texture, Thresholding, and Morphological Operations," Proc. IEEE International Conference on Electro/Information Technology (EIT), 1-6 (2011).
- [8] Oprea, S., Liță, I., Jurianu, M., Vișan, D.A., and Cioc, I.B., "Digital Image Processing Applied in Drugs Industry for Detection of Broken Aspirin Tablets," Proc. 31st International Spring Seminar on Electronics Technology (ISSE), 121-124 (2008).
- [9] Sarvaiya, J.N., Patnaik, S., and Bombaywala, S., "Image Resgistration by template matching using normalized cross-correlation," Proc. International Conference on Advances in Computing, Control, and Telecommunication Technologies (ACT), 819-822 (2009).



APPENDIX B

จุฬาลงกรณ์มหาวิทยาลัย
CHULALONGKORN UNIVERSITY

Program coding

Below is program coding for one column of rubber latex vessel detection and segmentation

```

rubber = imread('rt1.jpg');
rubber = imresize(rubber,[500 500]);
gray_rubber = rgb2gray(rubber);

he = histeq(gray_rubber);

[d1,d2] = size(gray_rubber);

J = gray_rubber;
bw_J = im2bw(he);
comple_J = imcomplement(bw_J);
J_fill = imfill(comple_J,'holes');
L = bwlabel(J_fill,4);
a=tabulate(L(:));

x = a(a(:,2)==max(a(2:end,2)),1);

[r,c] = find(L==x);
rc = [r c];
min_x = min(rc);

z = a(2:end,2);
x2 = a(a(:,2)==max(z(z ~= max(z))),1); %2nd max

[row2, col2] = find(L==x2);
rc2 = [row2 col2];
min_x2 = min(rc2);

[m,n] = size(L);

J_new = gray_rubber;

for i=1:m
    for j=1:n
        if L(i,j) ~= x
            J_new(i,j)=255;

```



```

        end

    end
end

se = strel('disk',1);
result = imerode(J_new,se);

v_rubber = result;
[row,col,v] = find(v_rubber);

mean_v = mean(v);

max_v = max(max(v));
min_v = min(min(v));
avg_v = (max_v+min_v)/2;

[d1,d2] = size(v_rubber);

for i=1:d1
    for j=1:d2
        if v_rubber(i,j) > avg_v
            v_rubber(i,j)=255;
        end
    end
end

figure,imshow(v_rubber);

col_v = v_rubber(1:end,1);
figure,imshow(col_v);

[m,n] = size(v_rubber);
figure,plot(1:m,col_v, '.');

co_d = im2double(col_v);
co_d = co_d*255;

ro = (1:1:m);
ro = transpose(ro);

p = polyfit(ro,co_d,10);
pv = polyval(p,ro);

figure, plot(col_v, '.'); hold on; plot(pv);

mean_data = mean(col_v);
new_data = find(col_v <= mean_data);

[fpeak,locs]=findpeaks(-pv);

fpeak = fpeak*(-1);

```



```

col_vnew = col_v;

min_fpeak = min(fpeak);
min2_fpeak = min(fpeak (fpeak ~= min_fpeak));

locs_min = find(fpeak == min_fpeak);
locs_min2 = find(fpeak == min2_fpeak);

co_min = locs(locs_min);
co_min2 = locs(locs_min2);

[fpeak_max, locs_max]=findpeaks(pv);

new_pv = floor(pv);

mean_pv = mean(pv);
f_meanpv = find(fpeak <= mean_pv);
locs_fmean = locs(f_meanpv);
max_lfmean = max(locs_fmean);

if size(f_meanpv) == 1
else
A=0;
B=0;

for l = 1:length(locs_max)-1
    if( max_lfmean >= locs_max(l) && max_lfmean <= locs_max(l+1))
        A = locs_max(l);
        B = locs_max(l+1);
    end
end

for in = 1:A
    col_vnew(in) = 255;
end

end

figure, imshow(col_vnew);

```



APPENDIX C

จุฬาลงกรณ์มหาวิทยาลัย
CHULALONGKORN UNIVERSITY

Example results of rubber tree cross-sectional image data and Curve-fitting

Data RRIM600 (1rm.jpg)

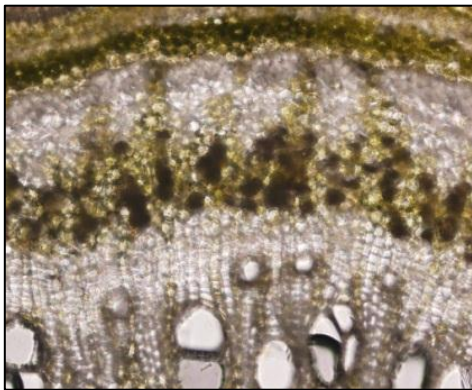


Figure 28: Original image 1rm.jpg

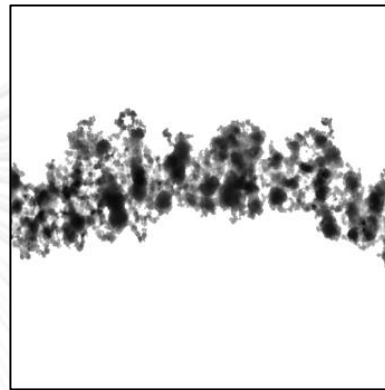


Figure 29: Segmentation Result of proposed method

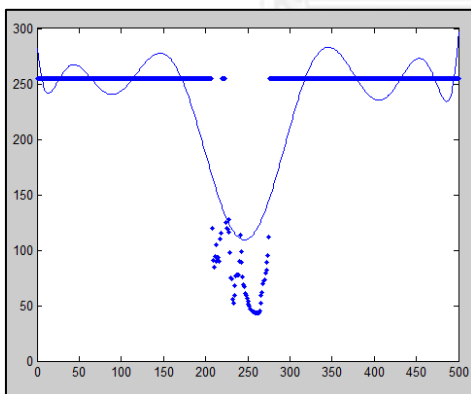


Figure 30: Plot of column 200 of original image

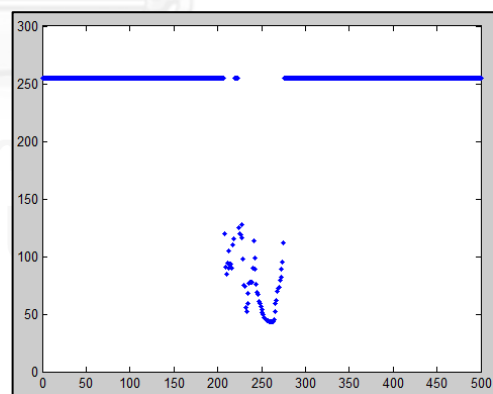


Figure 31: Plot of column 200 of segmentation result with proposed method

Data RRM600 (2rm.jpg)

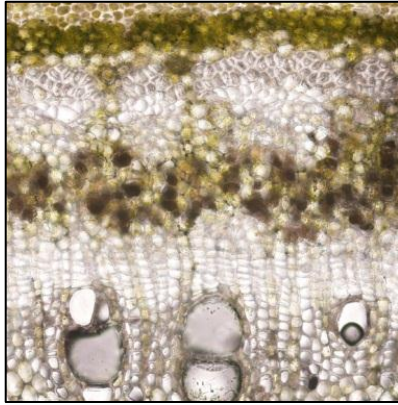


Figure 32: Original image 2rm.jpg

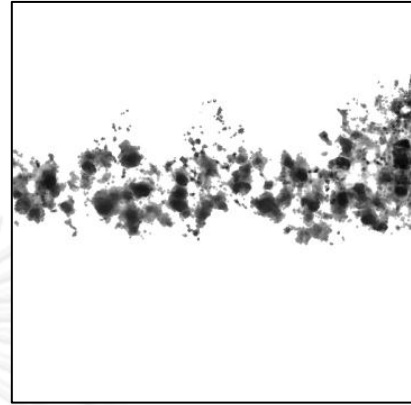


Figure 33: Segmentation Result
of proposed method

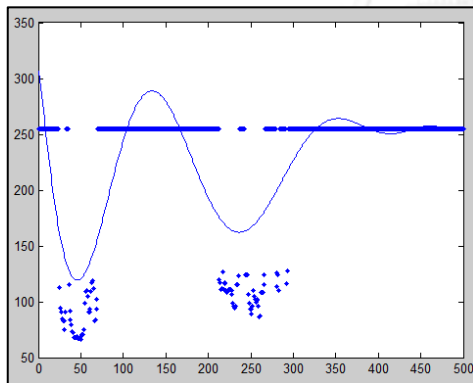


Figure 34: Plot of column 75 of
original image

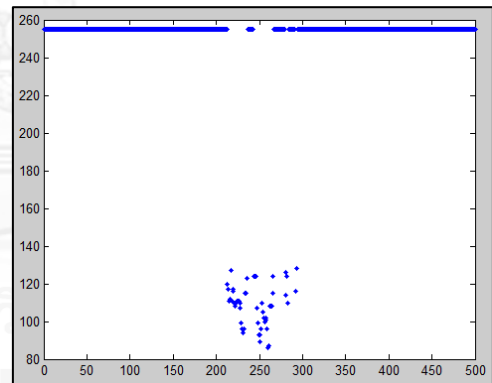


Figure 35: Plot of column 75 of
segmentation result with proposed
method

Data RRIM600 (4rm.jpg)

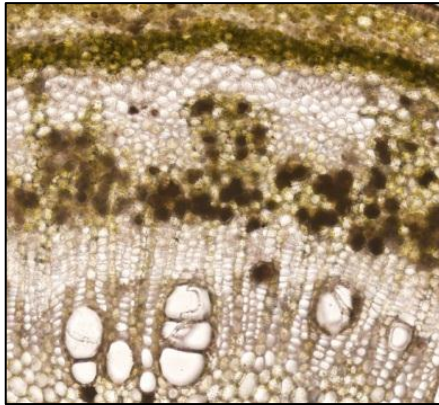
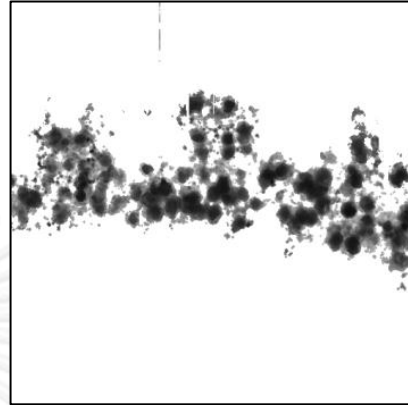
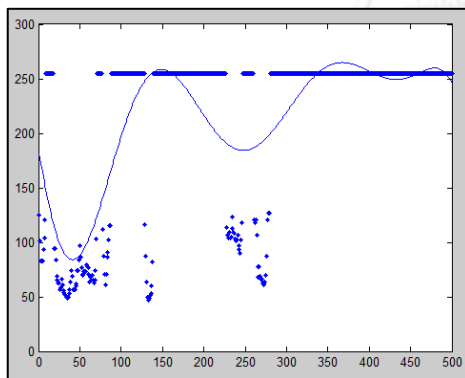
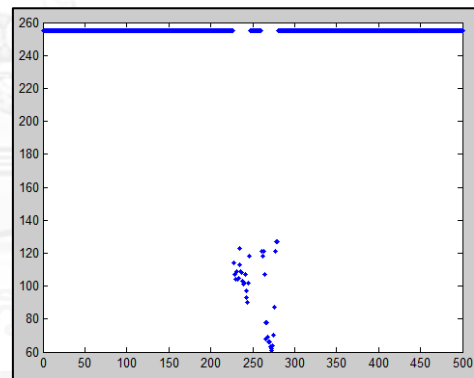


Figure 36: Original image 4rm.jpg

Figure 37: Segmentation Result
of proposed methodFigure 38: Plot of column 150 of
original imageFigure 39: Plot of column 150 of
segmentation result with proposed
method

Data RRIM600 (11rm.jpg)

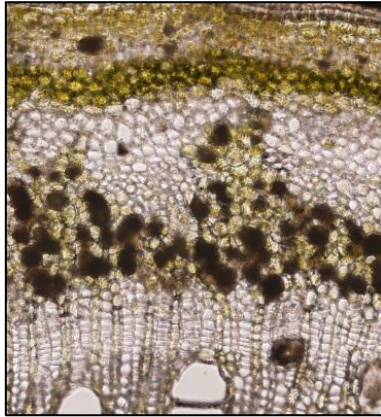


Figure 40: Original image
11rm.jpg

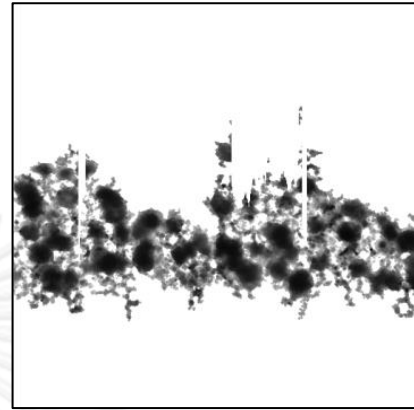


Figure 41: Segmentation Result of
proposed method

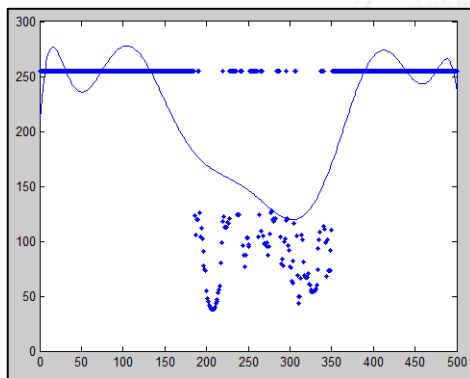


Figure 42: Plot of column 90 of
original image

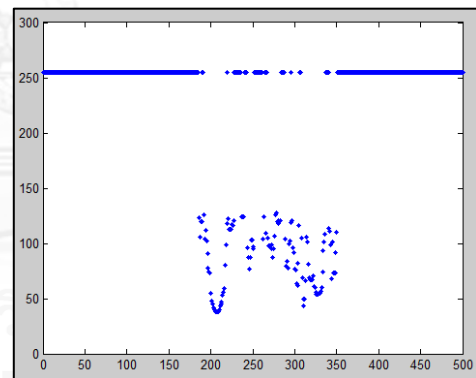


Figure 43: Plot of column 90 of
segmentation result with proposed
method

Data RRIM600 (26rm.jpg)



Figure 44: Original image 26rm.jpg

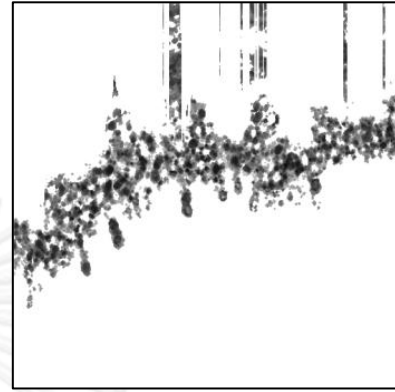


Figure 45: Segmentation Result of proposed method

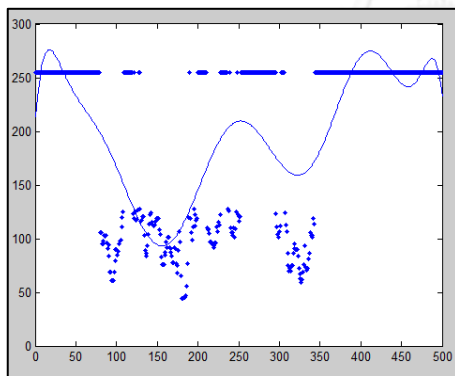


Figure 46: Plot of column 30 of original image

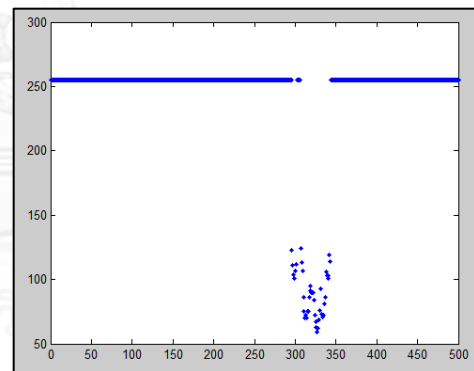


Figure 47: Plot of column 30 of segmentation result with proposed method

Data RRIM600 (29m.jpg)

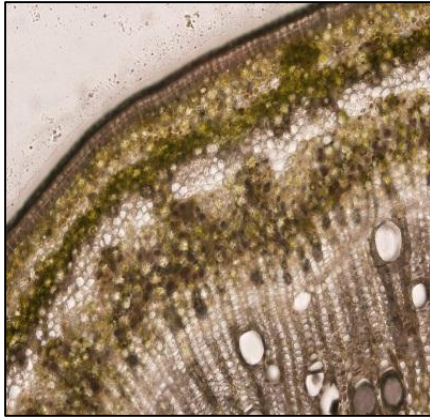


Figure 48: Original image 29m.jpg

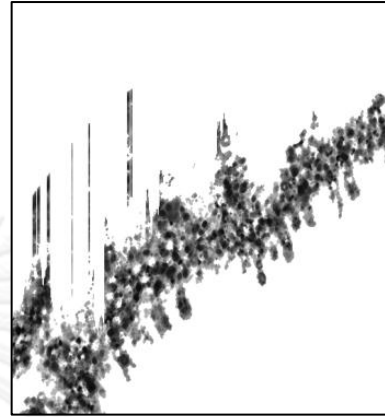


Figure 49: Segmentation Result of proposed method

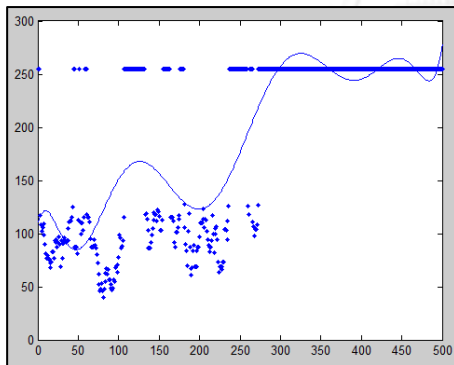


Figure 50: Plot of column 400 of original image

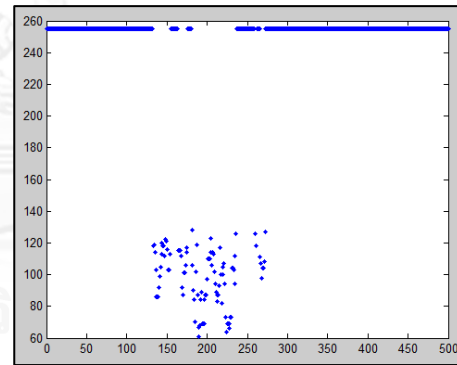


Figure 51: Plot of column 400 of segmentation result with proposed method

Data RRIT251 (rt1.jpg)

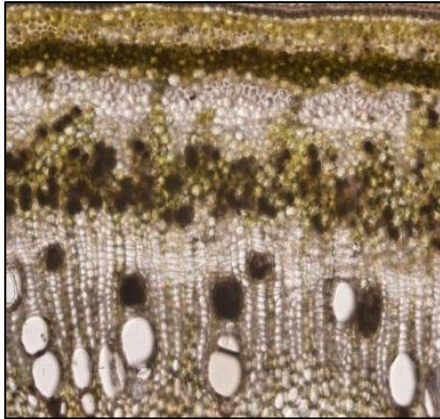


Figure 52: Original image rt1.jpg

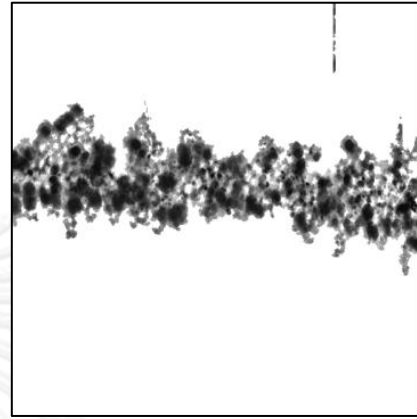


Figure 53: Segmentation Result of proposed method

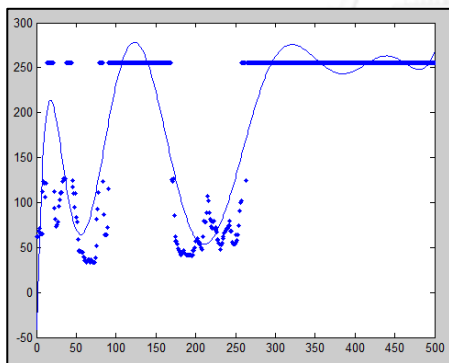


Figure 54: Plot of column 120 of original image

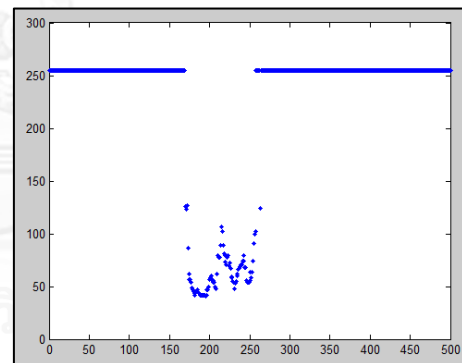


Figure 55: Plot of column 120 of segmentation result with proposed method

Data RRIT251 (rt3.jpg)

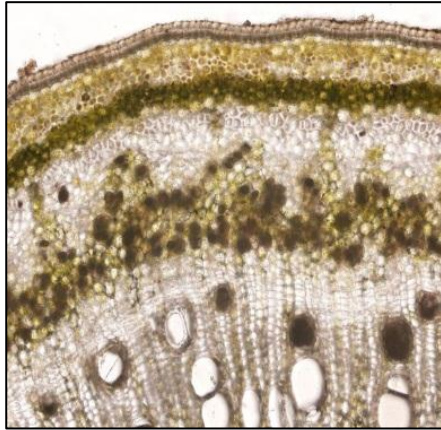


Figure 56: Original image rt3.jpg

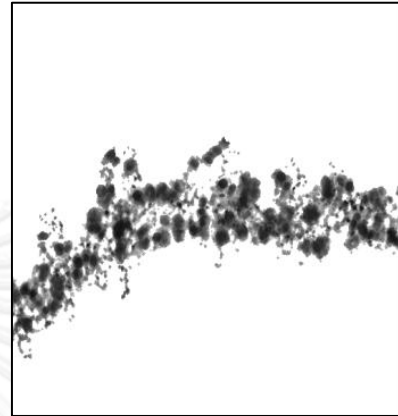


Figure 57: Segmentation Result of proposed method

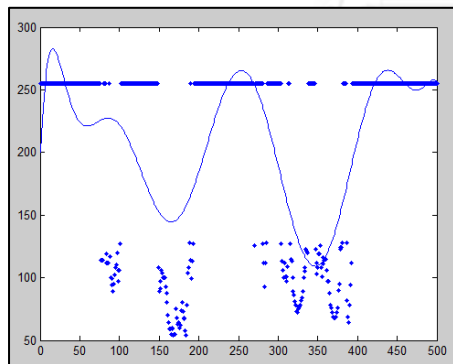


Figure 58: Plot of column 50 of original image

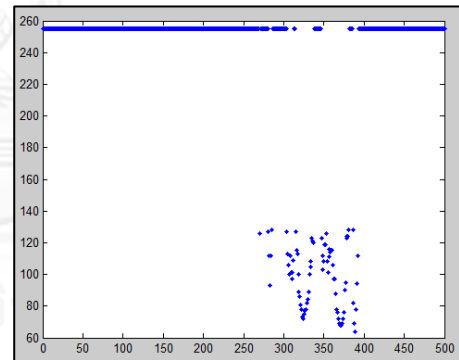


Figure 59: Plot of column 50 of segmentation result with proposed method

Data RRIT251 (rt4.jpg)

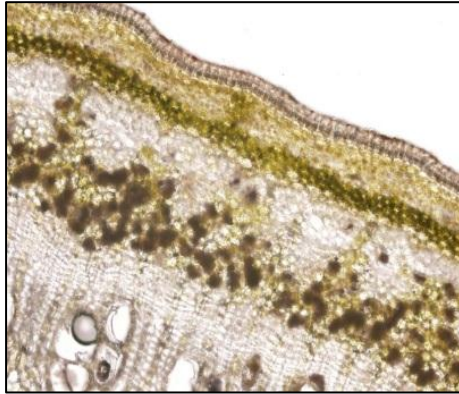


Figure 60: Original image rt4.jpg

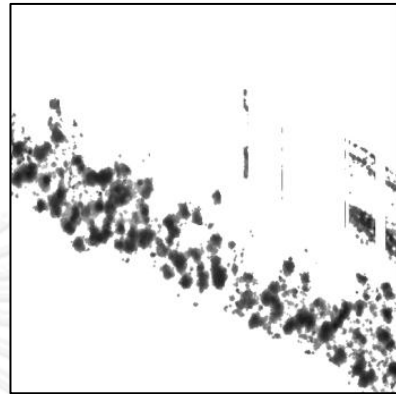


Figure 61: Segmentation Result of proposed method

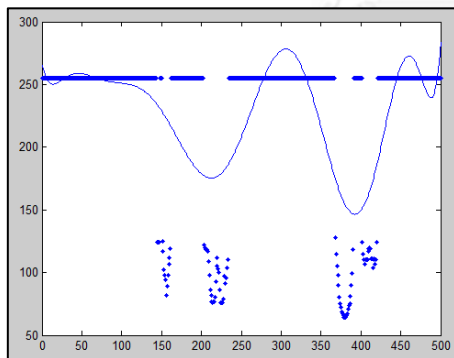


Figure 62: Plot of column 330 of original image

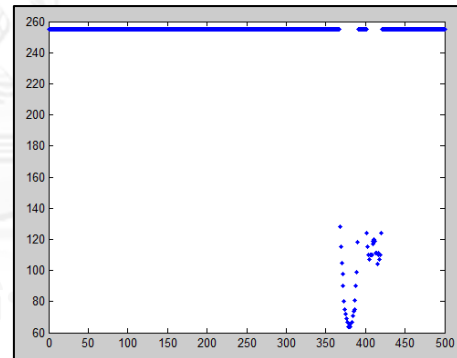


Figure 63: Plot of column 330 of segmentation result with proposed method

Data RRIT251 (rt7.jpg)

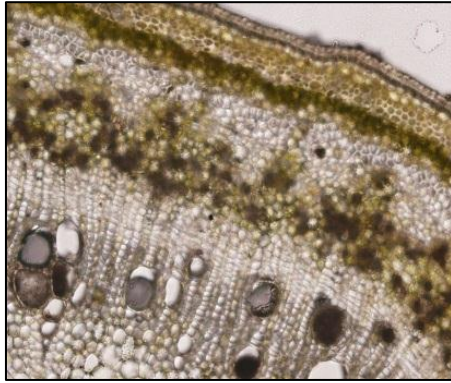


Figure 64: Original image rt7.jpg

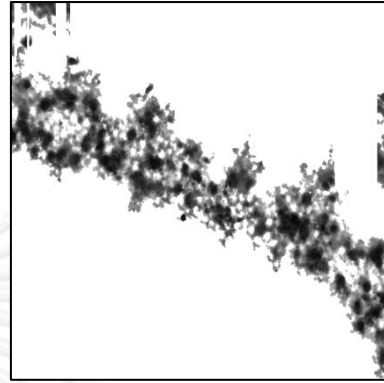


Figure 65: Segmentation Result
of proposed method

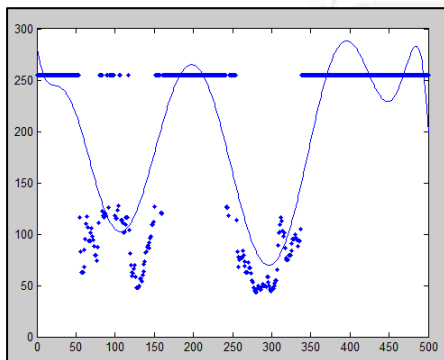


Figure 66: Plot of column 360 of
original image

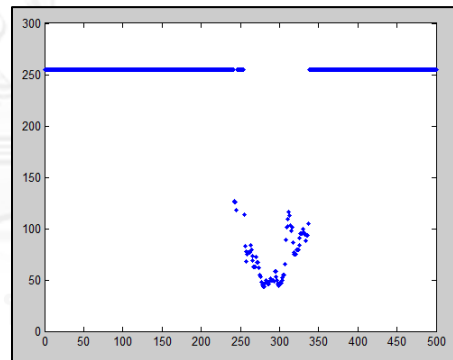


Figure 67: Plot of column 360 of
segmentation result with proposed
method

Data RRIT251 (rt9.jpg)

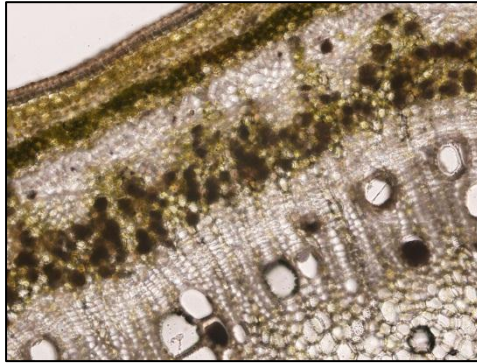


Figure 68: Original image rt9.jpg

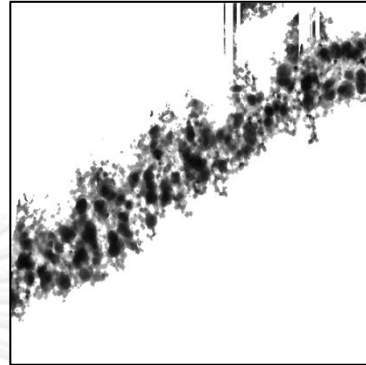


Figure 69: Segmentation
Result of proposed method

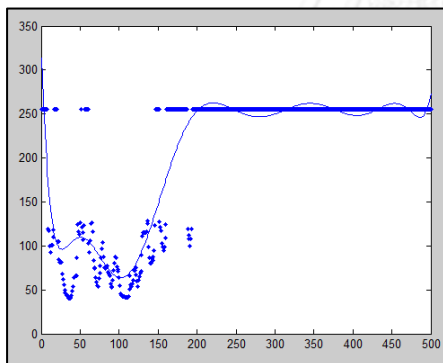


Figure 70: Plot of column 426 of
original image

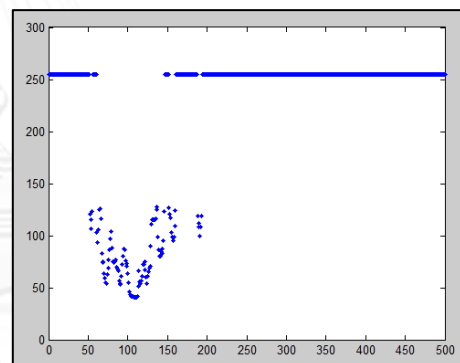


Figure 71: Plot of column 426 of
segmentation result with proposed
method

Data RRIT251 (rt21.jpg)

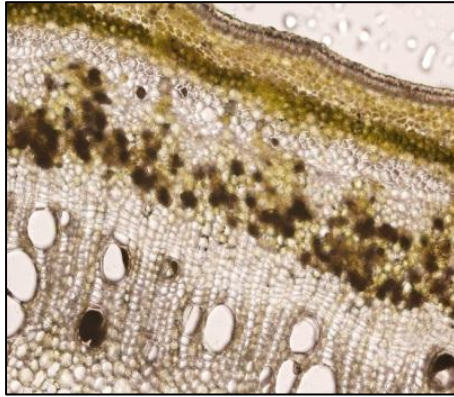


Figure 72: Original image rt21.jpg

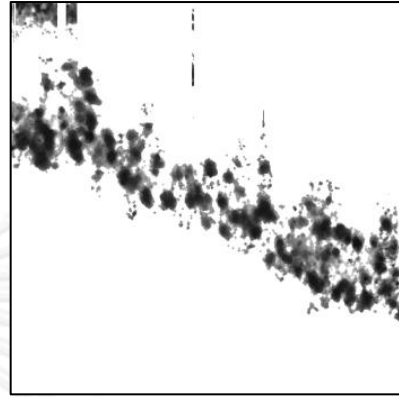


Figure 73: Segmentation Result of proposed method

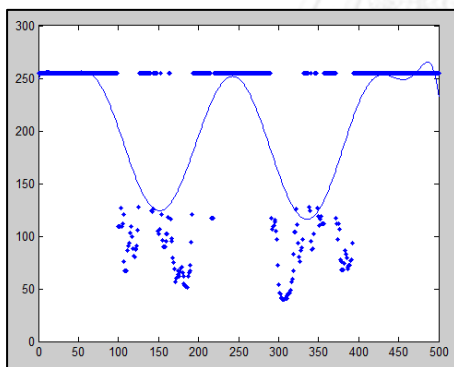


Figure 74: Plot of column 444 of original image

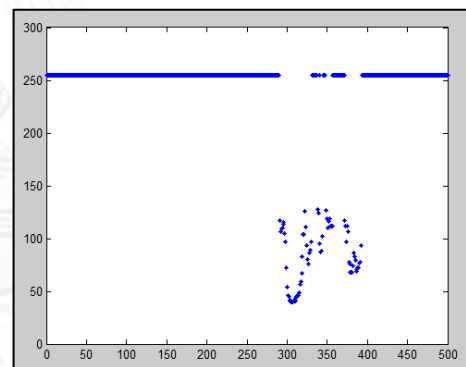


Figure 75: Plot of column 444 of segmentation result with proposed method

Example result of wrong detection and segmentation of rubber tree cross-sectional image data and Curve-fitting

Data RRIM600 (7rm.jpg)



Figure 76: Original image
7rm.jpg

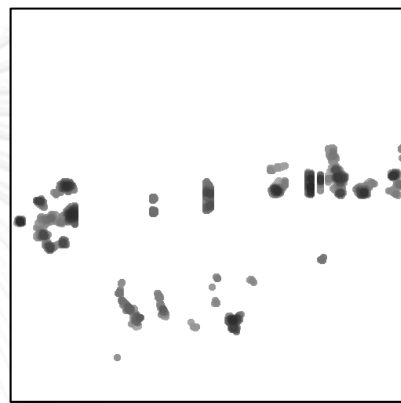


Figure 77: Segmentation Result
of proposed method

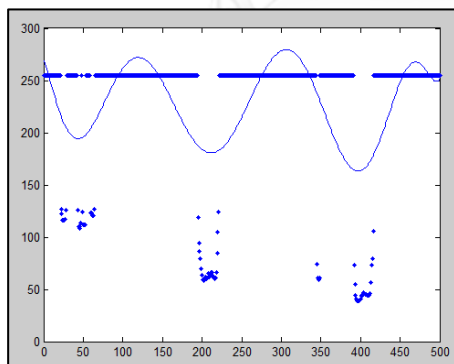


Figure 78: Plot of column 284 of
original image

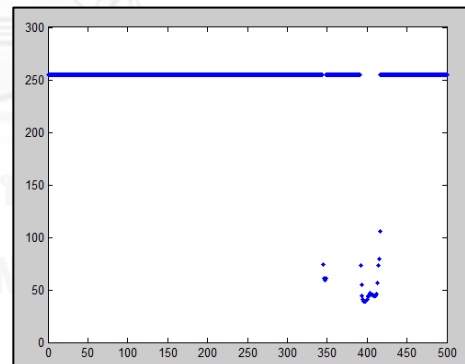


Figure 79: Plot of column 284 of
segmentation result with proposed
method

Data RRIT251 (rt25.jpg)

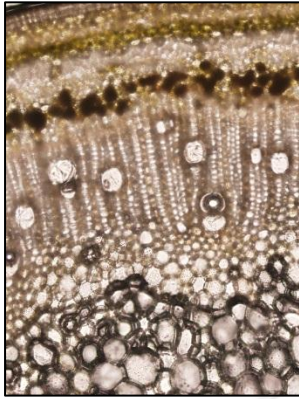


Figure 80: Original image
rt25.jpg

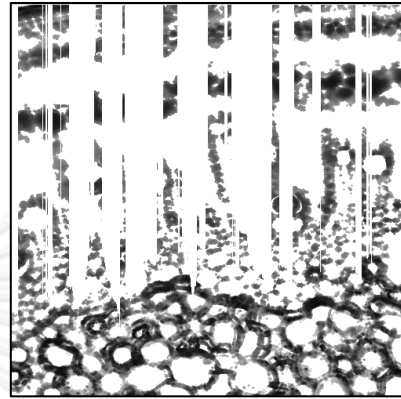


Figure 81: Segmentation Result
of proposed method

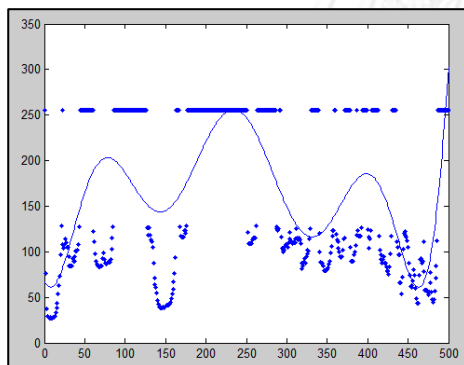


Figure 82: Plot of column 20 of
original image

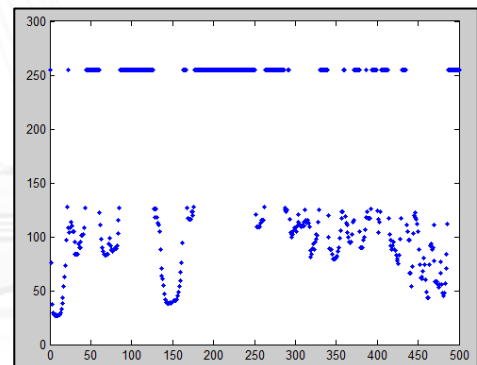


Figure 83: Plot of column 20 of
segmentation result with proposed
method

VITA

Ms.Jirapath Jariyawatthananon was born on November 25th, 1986, in Bangkok, Thailand. She has got a Bachelor degree in computer science from Sirindhorn international institute of technology, Thammasat university in 2009.

